**Naval Research Laboratory**
Washington, DC 20375-5320

NRL/MR/6401--00-8432

# DDG-51 FLT-IIA Airwake Study Part 3: Temperature Field Analysis for Baseline and Upgrade Configurations

ALEXANDRA LANDSBERG
WILLIAM C. SANDBERG

*Laboratory for Computational Physics & Fluid Dynamics*

April 17, 2000

# REPORT DOCUMENTATION PAGE

*Form Approved*
*OMB No. 0704-0188*



| 1. AGENCY USE ONLY (*Leave Blank*) | 2. REPORT DATE | 3. REPORT TYPE AND DATES COVERED |
|---|---|---|
| | April 17, 2000 | Memorandum Report |

**4. TITLE AND SUBTITLE**

DDG-51 FLT-IIA Airwake Study Part 3: Temperature Field Analysis for Baseline and Upgrade Configurations

**5. FUNDING NUMBERS**

**6. AUTHOR(S)**

Alexandria Landsberg and William C. Sandberg

**7. PERFORMING ORGANIZATION NAME(S) AND ADDRESS(ES)**

Naval Research Laboratory
Washington, DC 20375-5320

**8. PERFORMING ORGANIZATION REPORT NUMBER**

NRL/MR/6401--00-8432

**9. SPONSORING/MONITORING AGENCY NAME(S) AND ADDRESS(ES)**

Naval Sea Systems Command
2531 Jefferson Davis Hwy (SEA OIT)
Arlington, VA 22242-5160

**10. SPONSORING/MONITORING AGENCY REPORT NUMBER**

**11. SUPPLEMENTARY NOTES**

**12a. DISTRIBUTION/AVAILABILITY STATEMENT**

Approved for public release; distribution unlimited.

**12b. DISTRIBUTION CODE**

**13. ABSTRACT** (*Maximum 200 words*)

The FAST3D flow solver was used to analyze the unsteady temperature field for a baseline configuration and a proposed upgrade configuration for the DDG-51 Flt-IIA destroyer. The upgrade configuration was proposed to reduce IR signature without impacting other systems, particularly sensitive electronic equipment. The goal of this computational study was to analyze the unsteady temperature field for the proposed upgrade configuration and identify areas of concern. Comparison are made to the current baseline configuration, since neither experimental nor full-scale data are available.

**14. SUBJECT TERMS**

Unsteady fluid dynamics; Ship airwakes; Stack gas temperatures; Stack gas plume trajectories; Ship topside design simulation

**15. NUMBER OF PAGES**

34

**16. PRICE CODE**

| 17. SECURITY CLASSIFICATION OF REPORT | 18. SECURITY CLASSIFICATION OF THIS PAGE | 19. SECURITY CLASSIFICATION OF ABSTRACT | 20. LIMITATION OF ABSTRACT |
|---|---|---|---|
| UNCLASSIFIED | UNCLASSIFIED | UNCLASSIFIED | UL |

NSN 7540-01-280-5500

Standard Form 298 (Rev. 2-89)
Prescribed by ANSI Std 239-18
298-102

# DDG-51 Flt-IIA Airwake Study
# Part 3: Temperature Field Analysis for Baseline and Upgrade Configurations

**A. Landsberg and W. C. Sandberg**
**Laboratory for Computational Physics and Fluid Dynamics**
**Naval Research Laboratory**
**Washington, DC 20375-5344**

## 1. INTRODUCTION

The FAST3D flow solver was used to analyze the unsteady temperature field for a baseline configuration and a proposed upgrade configuration for the DDG-51 Flt-IIA destroyer. The upgrade configuration was proposed to reduce IR signature without impacting other systems, particularly sensitive electronic equipment. The goal of this computational study was to analyze the unsteady temperature field for the proposed upgrade configuration and identify areas of concern. Comparisons are made to the current baseline configuration, since neither experimental nor full-scale data are available.

## 2. BACKGROUND

The prior unsteady airwake computations for the DDG-51 Flt-IIA destroyer have been described by Landsberg, *et al.* [1,2,3]. Those studies examined the flow in the helicopter landing area, the effect of coupling helicopter rotor downwash, the temperature field on electronics, and the ingestion of stack gas into the hangars. Throughout these investigations we have generated time history data in order to provide, as a by-product for possible future needs, input for pilot training and landing platform evaluation using flight training simulators. The present effort continues the work but this time focusing on the effect of rather small design changes for infrared signature reduction. The accurate representation of complex geometry enables one to investigate the flow field differences

Manuscript approved February 24, 2000.

associated with changes to the design, such as stack geometry, uptake height, and the placement of electronic systems. The Virtual Cell Embedding approach [7,8] for the generation of structured meshes for complex shapes is the basis for this capability.

## 3. COMPUTATIONAL METHODS

These computations were carried out using the unsteady flow solver, FAST3D, developed at the Laboratory for Computational Physics and Fluid Dynamics (LCP&FD). FAST3D has the capability of modeling highly complex configurations in an efficient manner. A parallel processing computer is well-suited for performing these computations due to the large computational grid and the large number of time steps required to acquire the unsteady data. The FAST3D code is based upon the Flux-Corrected Transport (FCT) algorithm [4,5,6] with the virtual cell embedding (VCE) method [7,8].

A necessary modification for ship airwake calculations is the addition of an atmospheric boundary layer model. In order to represent the atmospheric boundary layer over the open ocean, the model by Davenport [8] was incorporated into FAST3D. The atmospheric boundary layer is approximated by the power-law profile

$$u/u_{ref} = \left(z/z_{ref}\right)^n$$

where $u_{ref}$ is a known velocity at a specified reference level $z_{ref}$. For the DDG-51 Flt-IIA simulations, $z_{ref}$ is taken as the location of the ship anemometer which is at a height of 44.5 m. According to Davenport, the index $n$ is usually found by matching the log- and power-law profiles at some appropriate elevation, yielding

$$n = 1/\ln\left(z_1/z_0\right)$$

Davenport gives the range of $0.01 > z_0 > 0.001$ for the roughness length scale in neutrally buoyant flow over the rough sea. A mean value of $z_0 = 0.005$ was chosen. An appropriate reference level ($z_1$) is the helicopter landing deck at a height of 10 m, which results in $n$ = 0.13. This atmospheric boundary layer profile is imposed at the inflow plane. The implementation allows any wind angle to be specified relative to the ship heading.

## 4. RESULTS AND DISCUSSION

The unsteady data analysis consists of time histories of the velocity components and stack gas

distribution, time-averaged velocity fluctuations, and power spectra of velocities at selected points of interest. To gain a better understanding of the global features of the airwake, two-dimensional slices of the flow quantities are presented.

### 4.1 DDG51 Problem Description

The FAST3D representation of the DDG-51 Flt-IIA is shown in Figure 1. The inset figure shows the CAD panel representation. Figure 2(a) is a close up view of the baseline configuration; Figure 2(b) shows the corresponding upgrade configuration. This analysis of the temperature field was performed to determine the effects of a design change in the stack casings of the DDG51. The primary design change in the upgrade configuration consists of lowering the stacks 5 feet to be flush with the casing. Additional modifications included making the aft stack flush with a casing and mounting a GBS system on top of this casing. Initially five locations, corresponding to the INMARSAT, TV@SEA, Director 2, Director 3 and the GBS were chosen for analysis. These locations are labeled in Figure 2(b). In a tail wind, electronic equipment on the mast could be affected by the exhaust plume. Therefore, for the tail wind simulation 6 antenna locations were included in the analysis plus one point in the plume along the centerline. Table I summarizes the designation of these points of interest and their locations. Near the INMARSAT and TV@SEA several points were analyzed to capture variations in the temperature field. The CFD results include (1) tables summarizing the mean, maximum and standard deviations of temperature, (2) snapshots of the three-dimensional temperature field and (3) time-accurate unsteady temperature histories. The temperature field is for the fluid surrounding the equipment and not the surface temperature of the equipment. There is no account for solar absorption or for heat emitted by the equipment.

The computational grid for this problem is 320 x 96 x 128 (axial, vertical, transverse) and is shown in Fig. 3(a). A close-up of the grid resolution near the main stacks is shown in Fig. 3(b). The grid resolution is 1/3 meter near the stacks. Fore and aft of the main stacks the grid resolution is 1 meter. Away from the superstructure, grid stretching was used to provide an adequate computational domain size. Three ship speed/wind speed and directions were performed: (i) 20 kt ship speed with a 20 kt wind speed at 0°, (ii) 20 kt ship speed with a 20 kt wind speed at 45°, and (iii) 14 kt ship speed with a 20 kt wind speed at 180°. The ambient temperature is specified as 100°F with an ambient density of 1.137 kg/m$^3$. There are two stack sizes, 8.5 ft. in diameter and 4 ft. in diameter. The larger stacks an exhaust temperature of 400°F and a density equal to 65% of the ambient density. The smaller stacks have a temperature of 325°F and a density equal to 73.6% of the ambient density. Buoyancy effects are included in the calculations via the density variations.

### 4.2 DDG51 Airwake Computations

CFD analysis of the temperature field was performed to determine the effects of a design change in the stack casings of the DDG51. The original design is termed 'baseline' while the new configuration is termed 'upgrade'. The primary design change in the upgrade configuration consists of lowering the stacks 5 feet to be flush with the casing.

A three-dimensional snapshot of temperature iso-contours is shown in Figs. 4(a) and 4(b) for the 20 kt ship speed with a 20 kt wind speed at 0°. The values of the temperature iso-contours were arbitrarily chosen at 125°F and 175°F. The 175°F temperature iso-contour is seen emanating from the stacks, rising slightly upward as well as showing some transverse motion (Fig. 4(b)). The 125°F temperature iso-contour shows that flow re-circulates forward of the stacks as well as getting pulled down onto the helicopter landing deck and moving downstream of the superstructure. A top-down view of temperature iso-contours at two different times is shown in Figs 5(a) and 5(b). The figures show that the flow field is highly unsteady and that temperatures of 125°F extend across the beam of the superstructure. The 175°F temperature iso-contour also shows significant movement in this time interval. The two lower figures, Figs. 5(c) and 5(d), show temperature iso-contours at 150°F and 250°F at the same two instances in time as Figs. 5(a) and 5(b), respectively. From these figures, one can conclude that most of the gases are at a temperature of 125°F and under for this set of conditions.

Several methods can be used illustrate a three-dimensional flow field. Particle path lines illustrate the unsteady flow field by tracking a series of particles in time. However, particle path lines increase the computational time as well as require significantly more memory. An alternate method to visualize the flow field is to plot streamlines. Streamlines assume the flow field has reached a steady state. For these unsteady calculations, if one saves the three-dimensional flow field at one instant in time, the streamlines can be plotted for this instant in time. Figures 6(a) and (b) show the streamlines at t=32 seconds for the 20 kt ship speed with a 20 kt wind speed at 0°. The streamlines are colored by velocity magnitude where blue is low and red is high. As one can see, the flow is undisturbed near the top of the mast; however near and aft of the stacks the flow is strongly affected by the superstructure and the emission of hot exhaust gases. Figs. 6(a) and (b) both show regions of slower flow between the two stack casings and over the helicopter landing deck. This is also illustrated in Fig. 6(a) where the two-dimensional plane shows velocity magnitude where blue is low and red is high. These figures qualitatively show the three-dimensional flow field. However, unsteady time histories are necessary to quantify the temperature field at desired locations. These are discussed next.

Table II shows a summary of the baseline and upgrade configuration at seven locations in terms of the mean temperature, maximum temperature and standard deviation during an 8 second interval

(corresponding to the time history plots from 24 second to 32 seconds). The mean temperature at these locations is consistently higher for the upgrade configuration with most of the equipment experiencing mean air temperatures around 130°F. This is approximately 10 °F higher than for the baseline configuration. In addition, the maximum temperatures experienced at these locations are also significantly higher for the upgrade configuration. The maximum temperature is experienced only once in the 8 second interval for a duration of approximately one half of a second. For this wind/ship speed condition, the air temperature surrounding the equipment increased for the upgrade configuratio,n, however the increase in mean temperature would appear not to significantly impact the electronic equipment.

For a ship speed of 20 kts with a 20 kt wind at 45°, only the upgrade configuration was analyzed. The results showed that the electronic equipment did not experience high temperatures and therefore analysis of the baseline configuration was not warranted. The mean, maximum and standard deviation of temperature at the equipment locations are shown in Table III. For this condition, the mean temperature was within 10°F of the ambient temperature at most locations. For both the headwind condition and the condition with a wind angle of 45°, the location most strongly impacted by the design modification is the aft stack/GBS which has a mean temperature of approximately 140°F-145°F for the upgrade configuration as compared to a mean temperature of 128°F for the baseline configuration. The time history plots at the aft stack/GBS show the instantaneous temperature is above 150°F for approximately 25% of the time interval sampled. We identify this location as an area where further analysis may be advisable to ensure satisfactory GBS performance.

The next condition analyzed is a ship speed of 14 kts with a 20 kt tailwind. This condition is more severe since the stack gases will get blown forward possibly effecting electronic equipment on the mast. A ship speed of 14 kts represents the most probable ship speed. For this condition, six additional points near the mast representing locations of the SPS-64, SPY-1 (port), SPY-1 (stbd), EHF, lower yardarm, and Ant. 6-7 were selected for analysis. One point in the plume was also chosen. Table IV shows the summary of the mean, maximum and standard deviation of temperature for the previous locations and the additional equipment locations on the mast. As one would expect, Directors 2 and 3 are not impacted by the tailwind. The mean and maximum temperature at these locations is lower for the upgrade configuration than the baseline configuration. The mean temperature near the location of the GBS is 150°F for the baseline configuration which is significantly higher than the upgrade configuration. For both configurations, the INMARSAT and TV@SEA have temperatures on the order of 120°F. It should be noted that for the headwind condition the air temperature near this equipment was of a similar magnitude. This is due to a recirculation in this region bringing warmer air forward of the stacks. The two areas most significantly impacted by the tailwind are near SPS-64 and Ant. 6-7. Near SPS-64, the baseline configuration has a mean temperature of 150°F while the upgrade configuration has a mean

temperature of 128°F. Similarly near Ant. 6-7 the baseline configuration has a mean temperature of 161°F while the upgrade configuration has a mean temperature of 139°F. The time history plots for both configurations show that the unsteady temperature field near Ant. 6-7 has many rapid repeated temperature spikes above 200°F, although the duration of these spikes is typically only one-quarter of a second to one-half of a second. These temperature spikes are indicative that Ant. 6-7 is near the edge of the hot gas plume, where the plume is moving in and away from the antennae. SPS-64 and Ant. 6-7 are at approximately the same height 104-105 feet ABL. These locations are in path of the plume. For the upgrade configuration, where the stacks are 5 feet lower, the plume does not rise as high as the baseline configuration and thus these locations are less heated. Similarly, the location labeled 'In Plume' in Table IV is in the path of the plume for the upgrade configuration (mean temperature = 220°F), but this location is below the path of the plume for the baseline configuration (mean temperature = 122°F). This tailwind condition indicates that some of the equipment may experience severe high temperatures. Analysis of the magnitude and duration of temperatures exceeding recommended operating levels may be advisable for equipment in the plume. Such an assessment would involve the probabilities of this operational condition occurring which would depend upon the ship speed-time-heading profile, the geographical locations of operation, and the meteorological probabilities for weather and wave conditions. Without access to the manufacturer's specifications for equipment temperature magnitude and duration limits, it is not possible for us to say if a complete probabalistic assessment of this sort is warranted.

## 5. SUMMARY AND CONCLUSIONS

Several computational fluid dynamics calculations were performed to compare the unsteady temperature field at selected locations for two topside configurations of the DDG51 Flt IIA destroyer. The upgrade configuration was proposed to reduce IR signature without impacting other systems including sensitive electronic equipment. The upgrade configuration has a GBS located near the aft stack. The results show that the GBS will, in certain operational conditions, experience average temperatures of 150°F and peak temperatures of 185°F. The performance of the GBS at these temperatures is not known. At Directors 2 and 3, the baseline and upgrade configurations showed average temperatures of 130°F or less. Short high temperatures spikes ( over 175°F) were experienced for a headwind condition. In the upgrade configuration, the INMARSAT and TV@SEA were placed flush with the stack casings. For a tailwind condition, these instruments can experience peak temperatures over 300°F. Based on discussions with the DDG51 Design Office, it was recommended that the INMARSAT and TV@SEA be lowered several feet to avoid being in the direct plume of the exhaust gases for tailwind conditions.

**Acknowledgments**

This work was supported by the NAVSEA DDG51 Design Office (Pat Crowe and Craig Bender).

## 6. REFERENCES

1. Landsberg, A.M., W.C. Sandberg, T.R. Young, Jr., and J.P. Boris, 1996, "DDG-51 Flt-IIA Airwake Study, Part 2: Hangar Interior Flow", Naval Research Laboratory Memorandum Report 96-7898, Washington, DC.

2. Landsberg, A.M., J.P. Boris., W.C. Sandberg, and T.R. Young, Jr., 1995, "Analysis of the Nonlinear Coupling of a Helicopter Downwash with an Unsteady Airwake", AIAA Paper 95-0047, American Institute of Aeronautics and Astronautics, Washington, DC.

3. Landsberg, A.M., J.P. Boris., W.C. Sandberg, and T.R. Young, Jr., 1993, "Naval Ship Superstructure Design: Complex Three-Dimensional Flows Using an Efficient Parallel Method", SCS Simulator Multiconference, San Diego, CA.

4. Boris, J.P. and D.L. Book, 1973. "Flux-Corrected Transport 1. SHASTA, A Fluid Transport Algorithm That Works." *J. Comput. Phys.* 11: 38-69.

5. Boris, J.P. and D.L. Book, 1976. "Solution of the Continuity Equation by the Method of Flux-Corrected Transport." Chapter 11 in *Methods in Computational Physics,* Academic Press, New York, 85-129.

6. Boris, J.P.; A.M. Landsberg; E.S. Oran; and J.H. Gardner, 1993. "LCPFCT - A Flux-Corrected Transport Algorithm for Solving Generalized Continuity Equations." NRL Memorandum Report 93-7192.

7. Landsberg, A.M.; J.P. Boris; T.R. Young, Jr.; and R.J. Scott, 1993. "Computing Complex Shocked Flows Through the Euler Equations." Proceedings of the 19th International Symposium on Shock Waves. Marseilles, France.

8. Young, Jr., T.R.; A.M. Landsberg; and J.P. Boris, 1993. "Implementation of the Full 3D FAST3D (FCT) Code Including Complex Geometry on the Intel iPSC/860 Parallel Computer." SCS Simulator Multiconference, San Diego, CA.

9. Davenport, A.G. 1982. *Engineering Meteorology*. E.J. Plate, Editor, Elsevier Scientific Publishing Company, Amsterdam, Netherlands, Chapter 12, 527-569.

| Designation | Location |
|---|---|
| | |
| INMARSAT-1 | 183', 6' port, 84' ABL |
| INMARSAT-2 | 186', 6' port, 84' ABL |
| INMARSAT-3 | 183', 6' port, 81' ABL |
| INMARSAT-4 | 186', 6' port, 81' ABL |
| | |
| TV@SEA-1 | 183', 4' stbd, 84' ABL |
| TV@SEA-2 | 186', 4' stbd, 84' ABL |
| TV@SEA-3 | 183', 4' stbd, 81' ABL |
| TV@SEA-4 | 186', 4' stbd, 81' ABL |
| | |
| Director 2 | 280', C/L, 83' ABL |
| Director 3 | 290', C/L, 77' ABL |
| Aft Stack/GBS | 380', 3' stbd, 58' ABL |
| | |
| SPS-64 | 156', 7.5' stbd, 105' ABL |
| SPY-1 (port) | 165', 22' port, 75' ABL |
| SPY-1 (stbd) | 165', 22' stbd, 75' ABL |
| EHF | 168', 12' stbd, 84' ABL |
| Lower Yardarm | 173', C/L, 120' ABL |
| Ant 6-7 | 174', C/L, 104' ABL |
| In Plume | 186', C/L, 87' ABL |

Table I. Designation and location of select points for temperature analysis.

| | TEMPERATURE | | | | | |
|---|---|---|---|---|---|---|
| | Baseline Configuration | | | Upgrade Configuration | | |
| Location | Mean | Max | Std. Dev. | Mean | Max | Std. Dev. |
| INMARSAT-1 | 121.8 | 134.5 | 5.3 | 128.3 | 160.1 | 9.1 |
| INMARSAT-2 | 120.5 | 129.5 | 5.9 | 138.6 | 250.1 | 26.8 |
| TV@SEA-1 | 119.7 | 131.4 | 5.5 | 127.7 | 187.1 | 13.8 |
| TV@SEA-2 | 118.5 | 162.0 | 9.0 | 128.9 | 351.6 | 42.5 |
| Director 2 | 128.3 | 237.0 | 24.8 | 128.6 | 252.7 | 27.2 |
| Director 3 | 116.1 | 130.7 | 6.2 | 133.0 | 212.0 | 25.8 |
| Aft Stack/GBS | 128.1 | 157.2 | 17.7 | 149.8 | 184.9 | 14.9 |

Table II. Mean, maximum and standard deviation of temperature given a 20 kt ship speed and 20 kt wind speed at 0°.

| | TEMPERATURE | | | | | |
|---|---|---|---|---|---|---|
| | Baseline Configuration | | | Upgrade Configuration | | |
| Location | Mean | Max | Std. Dev. | Mean | Max | Std. Dev. |
| INMARSAT-1 | - | - | - | 103.4 | 107.3 | 1.7 |
| INMARSAT-2 | - | - | - | 110.2 | 114.9 | 1.8 |
| TV@SEA-1 | - | - | - | 98.1 | 100.5 | 1.1 |
| TV@SEA-2 | - | - | - | 103.7 | 106.5 | 1.2 |
| Director 2 | - | - | - | 101.6 | 109.8 | 1.7 |
| Director 3 | - | - | - | 115.1 | 126.3 | 5.5 |
| Aft Stack/GBS | - | - | - | 141.0 | 185.8 | 17.2 |

Table III. Mean, maximum and standard deviation of temperature given a 20 kt ship speed and 20 kt wind speed at 45°.

| | TEMPERATURE | | | | | |
|---|---|---|---|---|---|---|
| | Baseline Configuration | | | Upgrade Configuration | | |
| Location | Mean | Max | Std. Dev. | Mean | Max | Std. Dev. |
| INMARSAT-1 | 117.4 | 135.7 | 3.2 | 120.0 | 193.7 | 11.5 |
| INMARSAT-2 | 117.5 | 130.1 | 3.4 | 124.9 | 318.9 | 25.8 |
| INMARSAT-3 | 117.8 | 128.6 | 2.8 | 117.1 | 135.3 | 3.6 |
| INMARSAT-4 | 118.2 | 128.6 | 2.8 | - | - | - |
| | | | | | | |
| TV@SEA-1 | 117.8 | 136.3 | 3.4 | 124.7 | 248.7 | 13.9 |
| TV@SEA-2 | 124.4 | 153.6 | 5.3 | 144.2 | 348.2 | 29.1 |
| TV@SEA-3 | 114.8 | 124.2 | 2.3 | 115.2 | 129.7 | 2.2 |
| TV@SEA-4 | 123.1 | 138.5 | 4.0 | 125.8 | 208.8 | 13.7 |
| | | | | | | |
| Director 2 | 105.2 | 152.6 | 12.4 | 102.9 | 138.0 | 8.2 |
| Director 3 | 110.8 | 170.7 | 14.7 | 108.3 | 150.2 | 12.4 |
| Aft Stack/GBS | 151.1 | 201.0 | 29.7 | 105.1 | 127.2 | 4.5 |
| | | | | | | |
| SPS-64 | 149.6 | 204.2 | 20.3 | 128.4 | 176.0 | 18.6 |
| SPY-1 (port) | 103.2 | 118.6 | 4.0 | 102.6 | 116.3 | 4.1 |
| SPY-1 (stbd) | 100.6 | 109.3 | 2.8 | 100.6 | 110.5 | 3.1 |
| EHF | 103.4 | 129.3 | 5.2 | 108.9 | 141.7 | 7.9 |
| Lower Yardarm | 99.9 | 110.3 | 1.6 | 99.4 | 107.2 | 0.9 |
| Ant 6-7 | 161.5 | 305.5 | 34.8 | 138.9 | 268.5 | 38.8 |
| In Plume | 121.0 | 144.6 | 4.0 | 218.3 | 378.6 | 60.2 |

Table IV. Mean, maximum and standard deviation of temperature given a 14 kt ship speed and 20 kt wind speed at 180°.

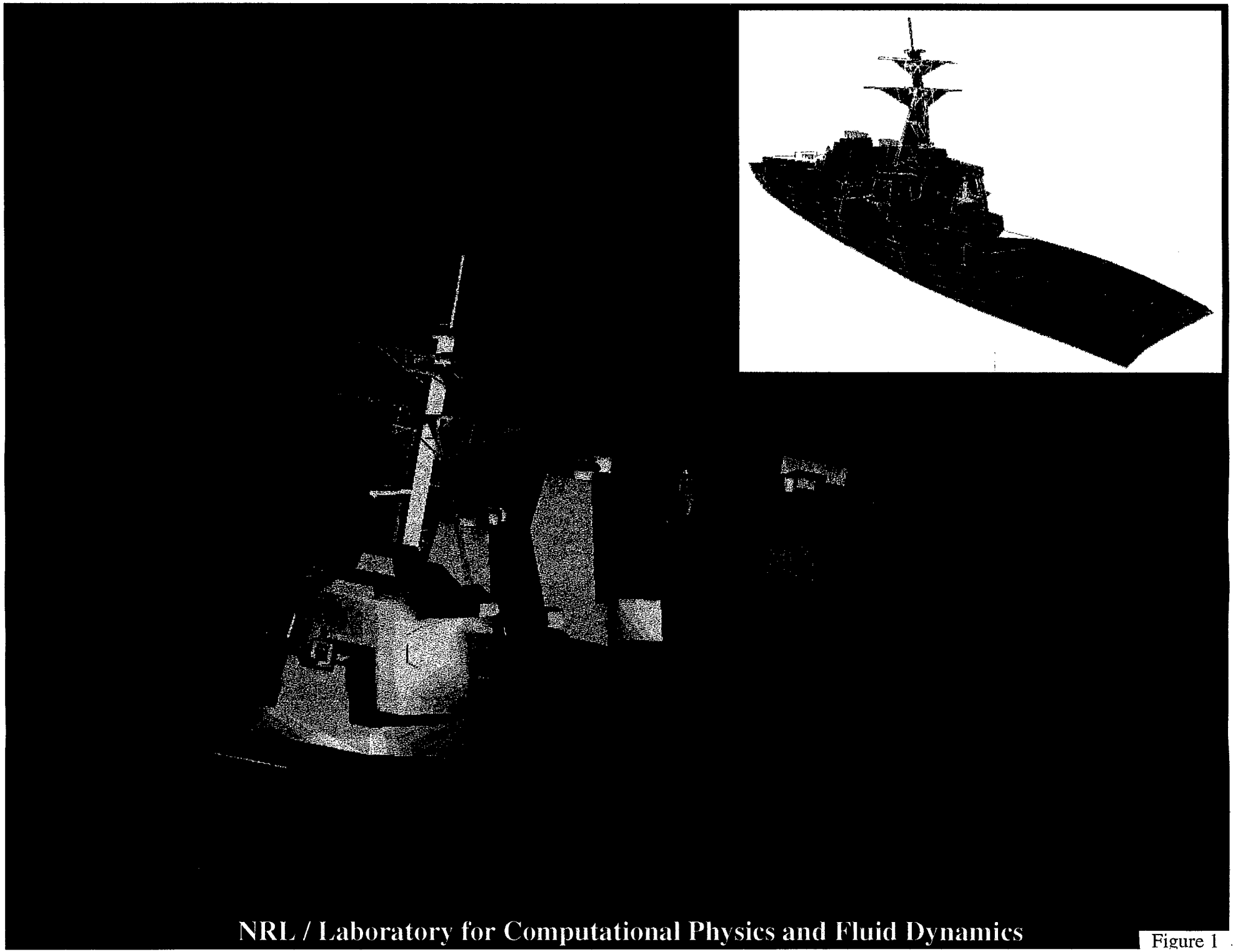
NRL / Laboratory for Computational Physics and Fluid Dynamics

Figure 1

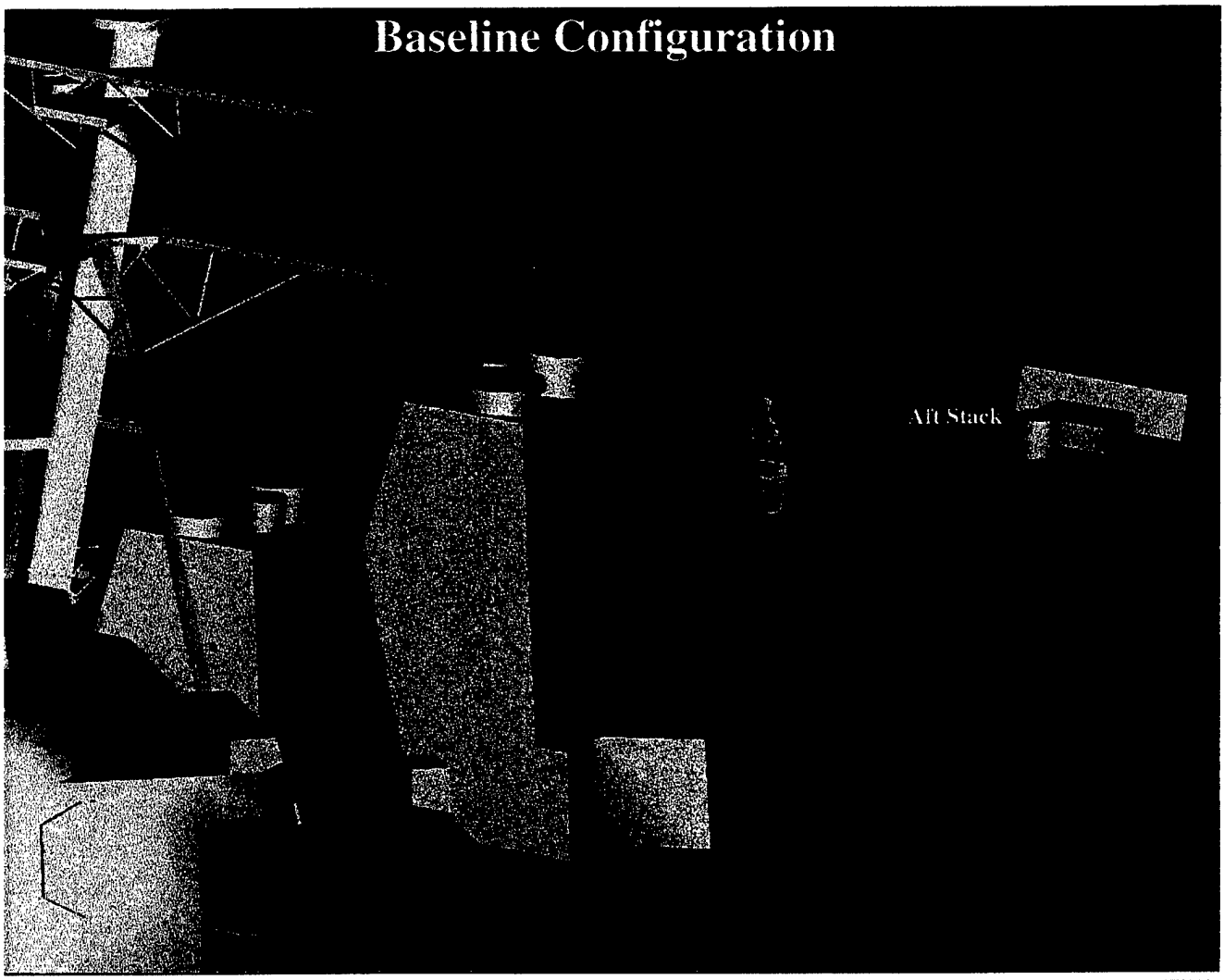
Baseline Configuration
Aft Stack

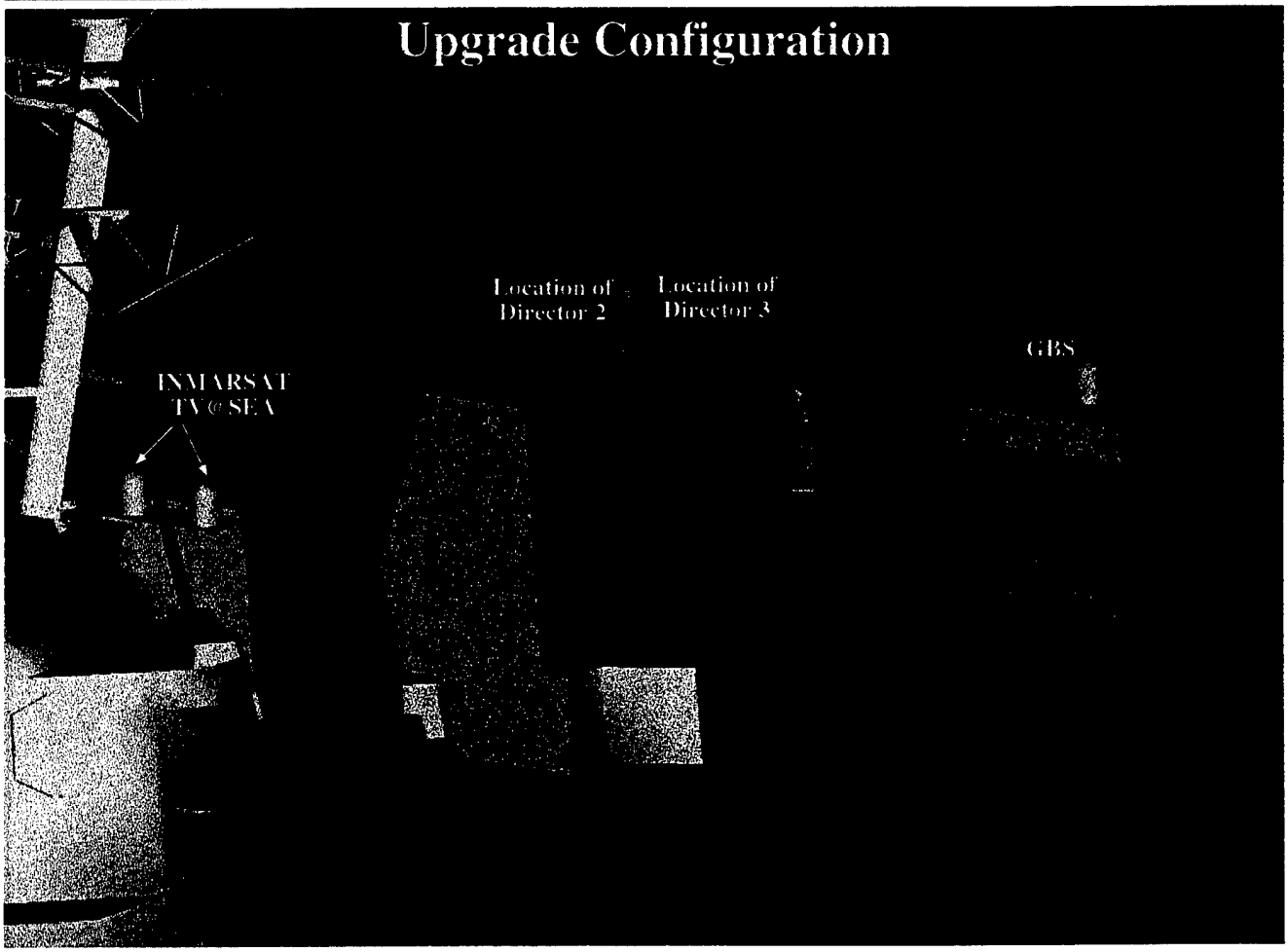
Upgrade Configuration
Location of Director 2
Location of Director 3
GBS
INMARSAT TV@SEA



Figure 2

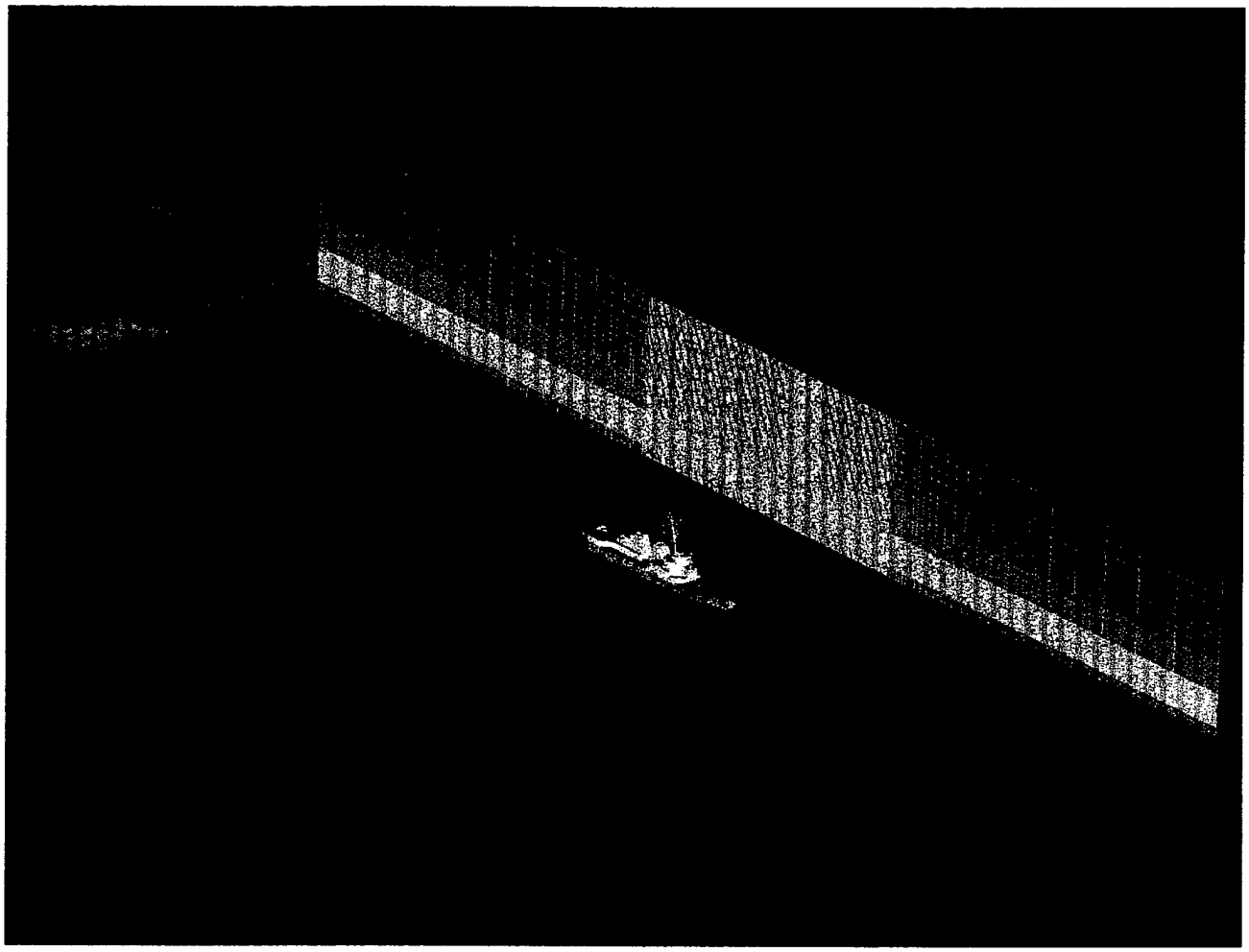

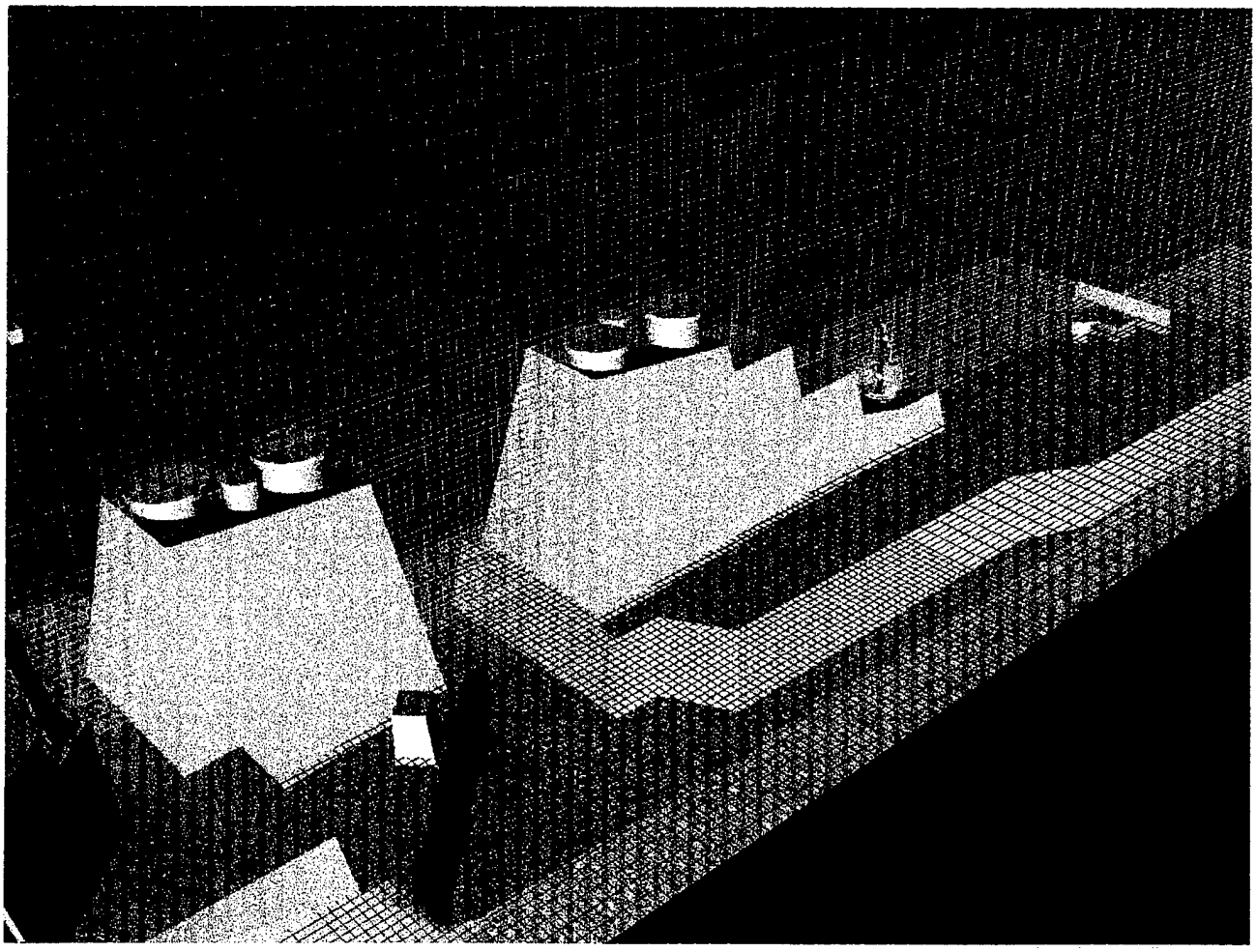

Figure 3

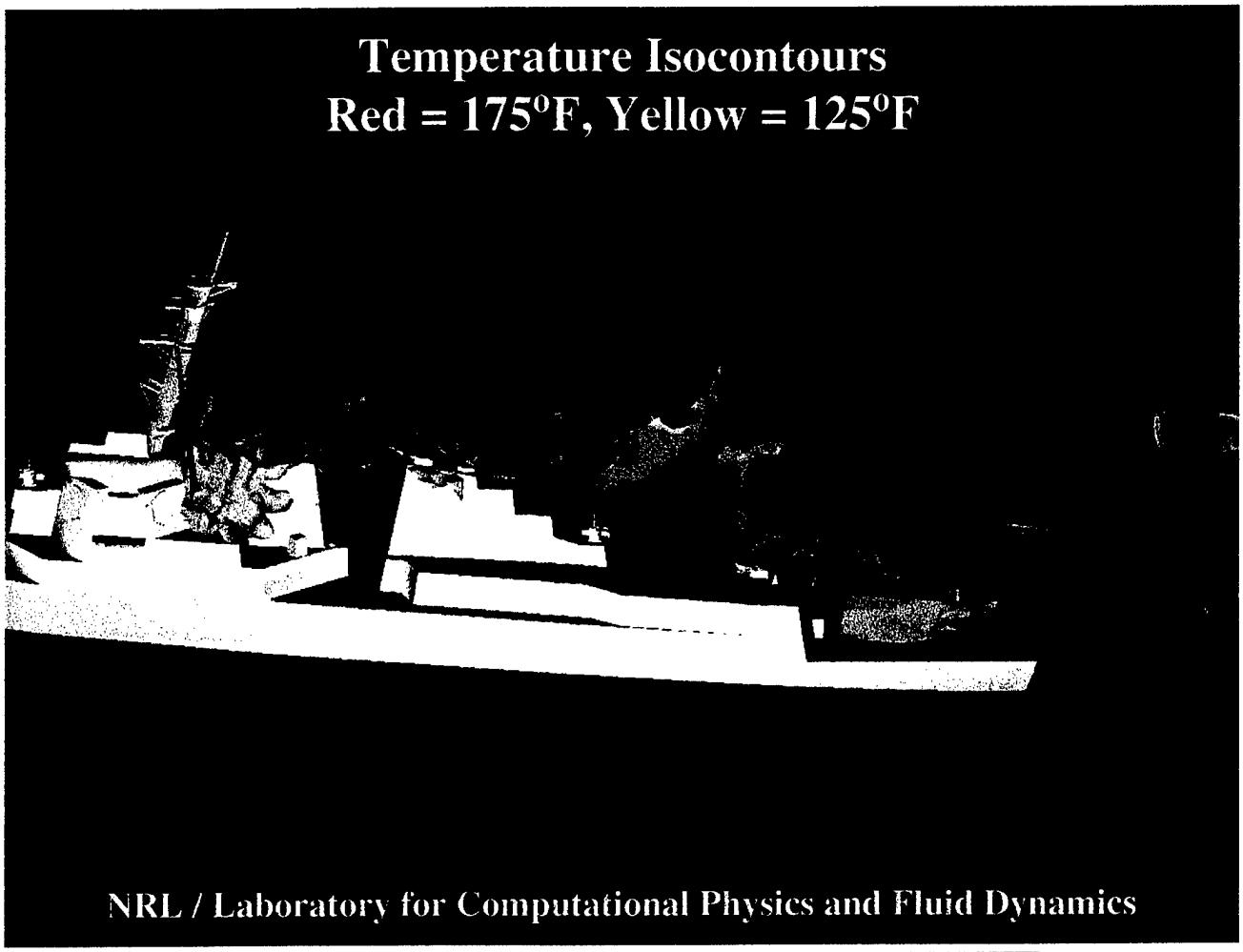
Temperature Isocontours
Red = 175°F, Yellow = 125°F
NRL / Laboratory for Computational Physics and Fluid Dynamics

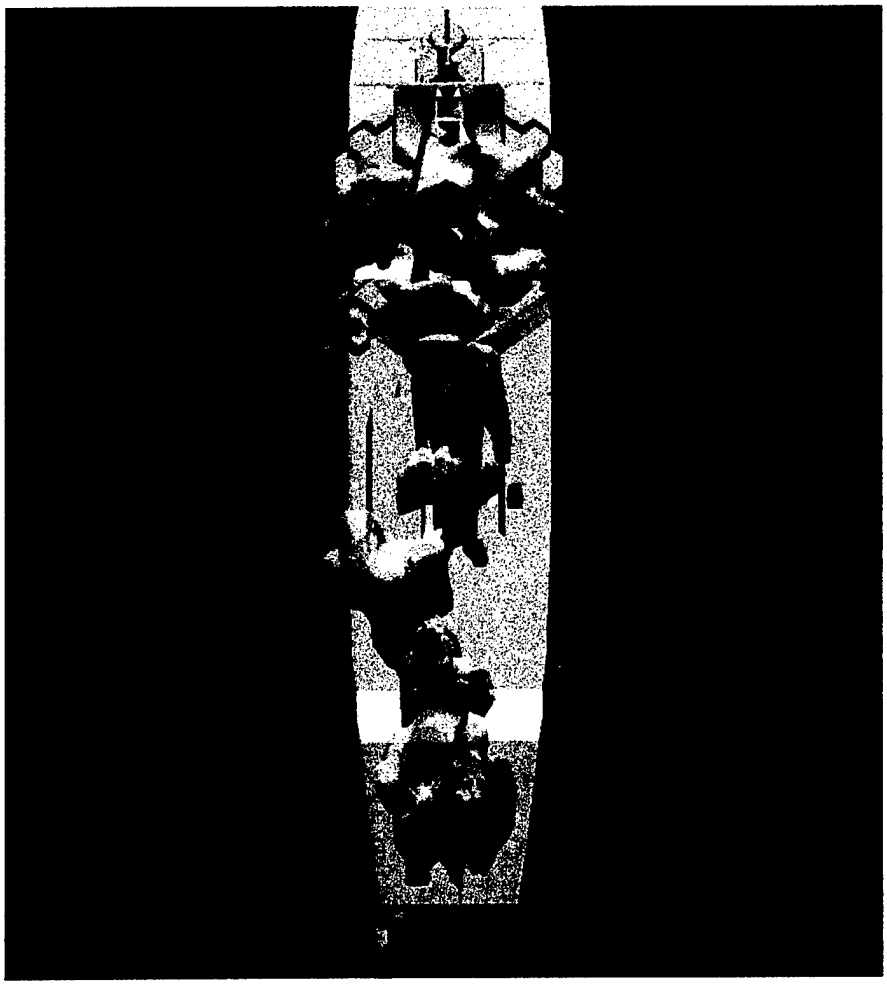

Figure 4

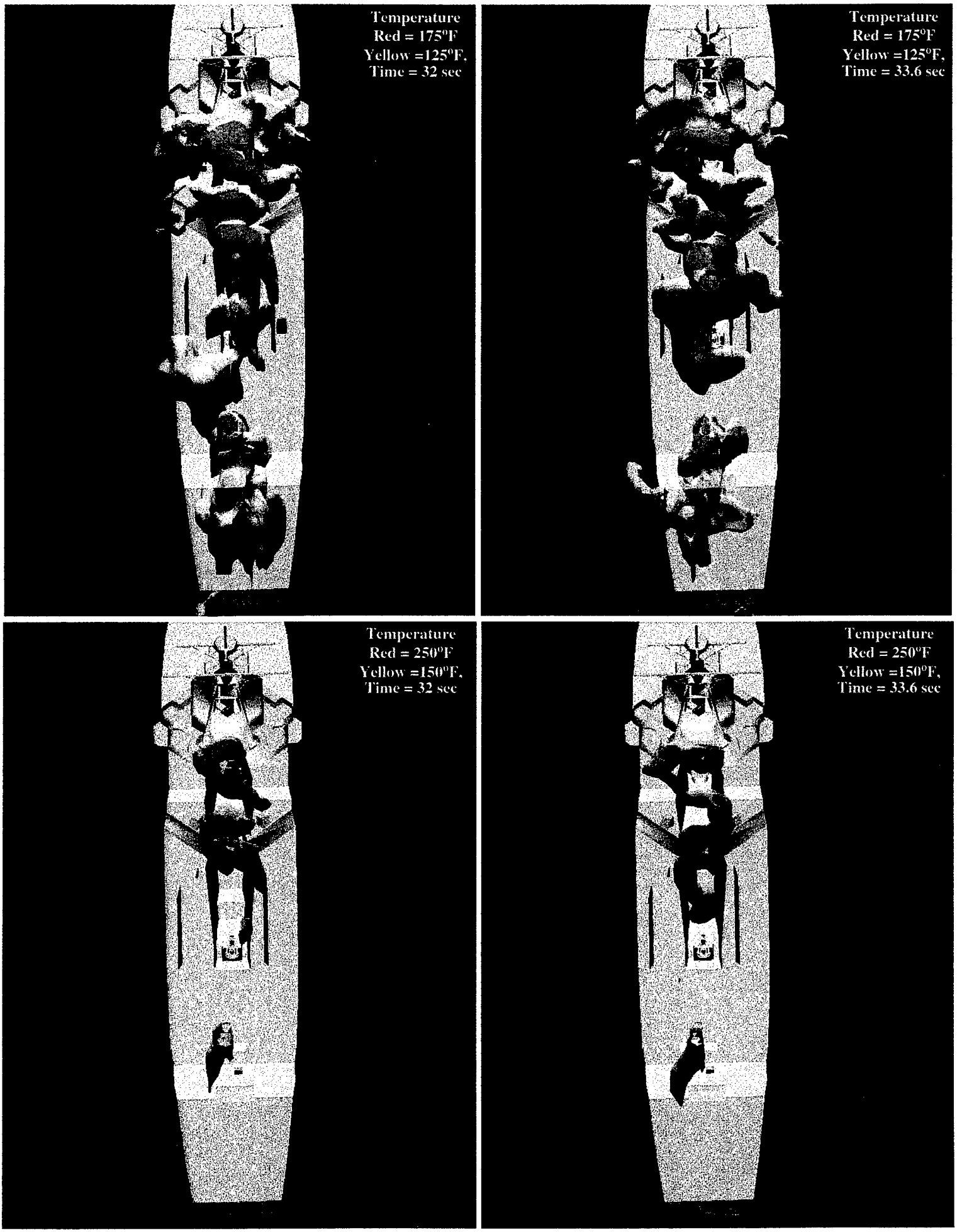


**NRL / Laboratory for Computational Physics and Fluid Dynamics** Figure 5

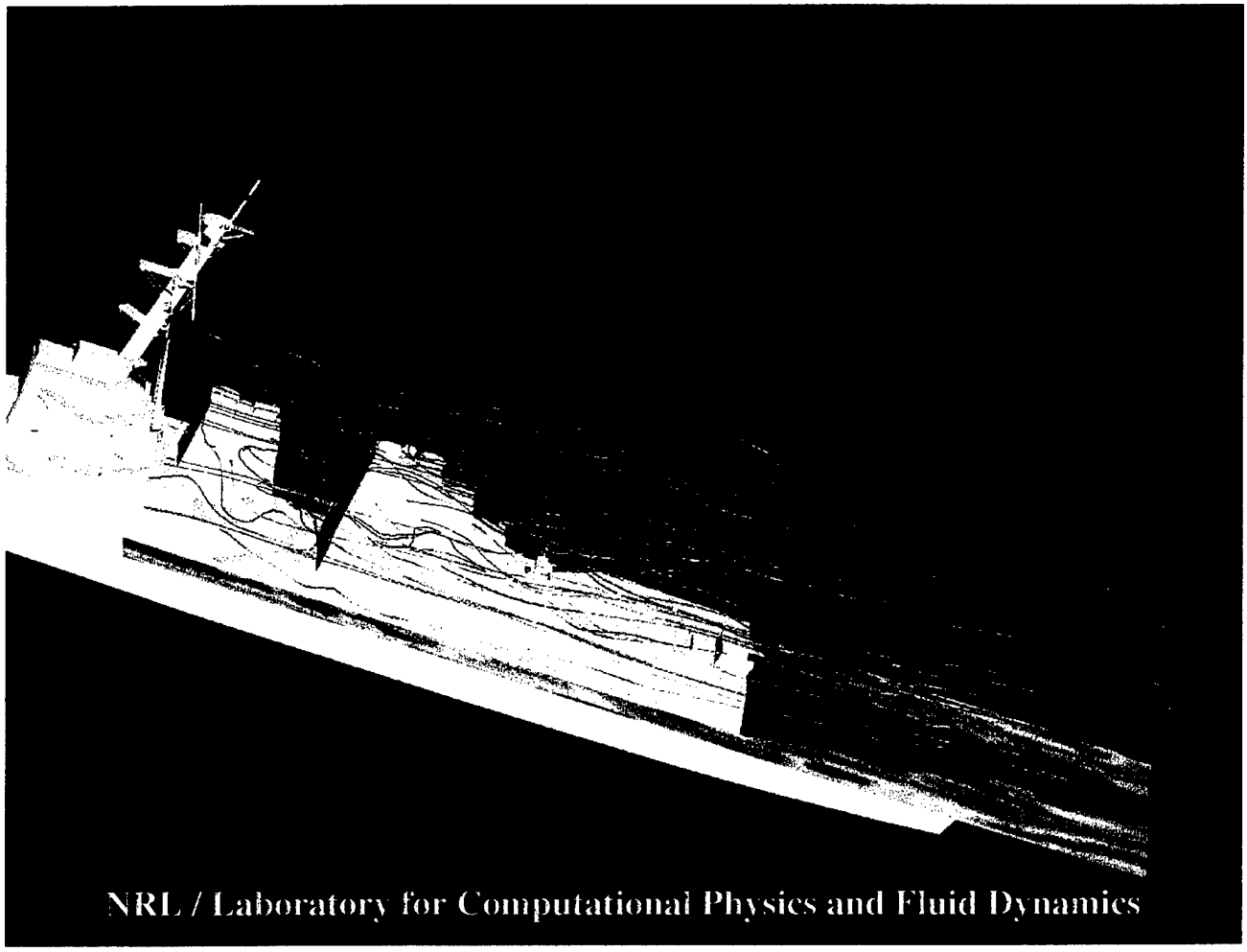
NRL / Laboratory for Computational Physics and Fluid Dynamics

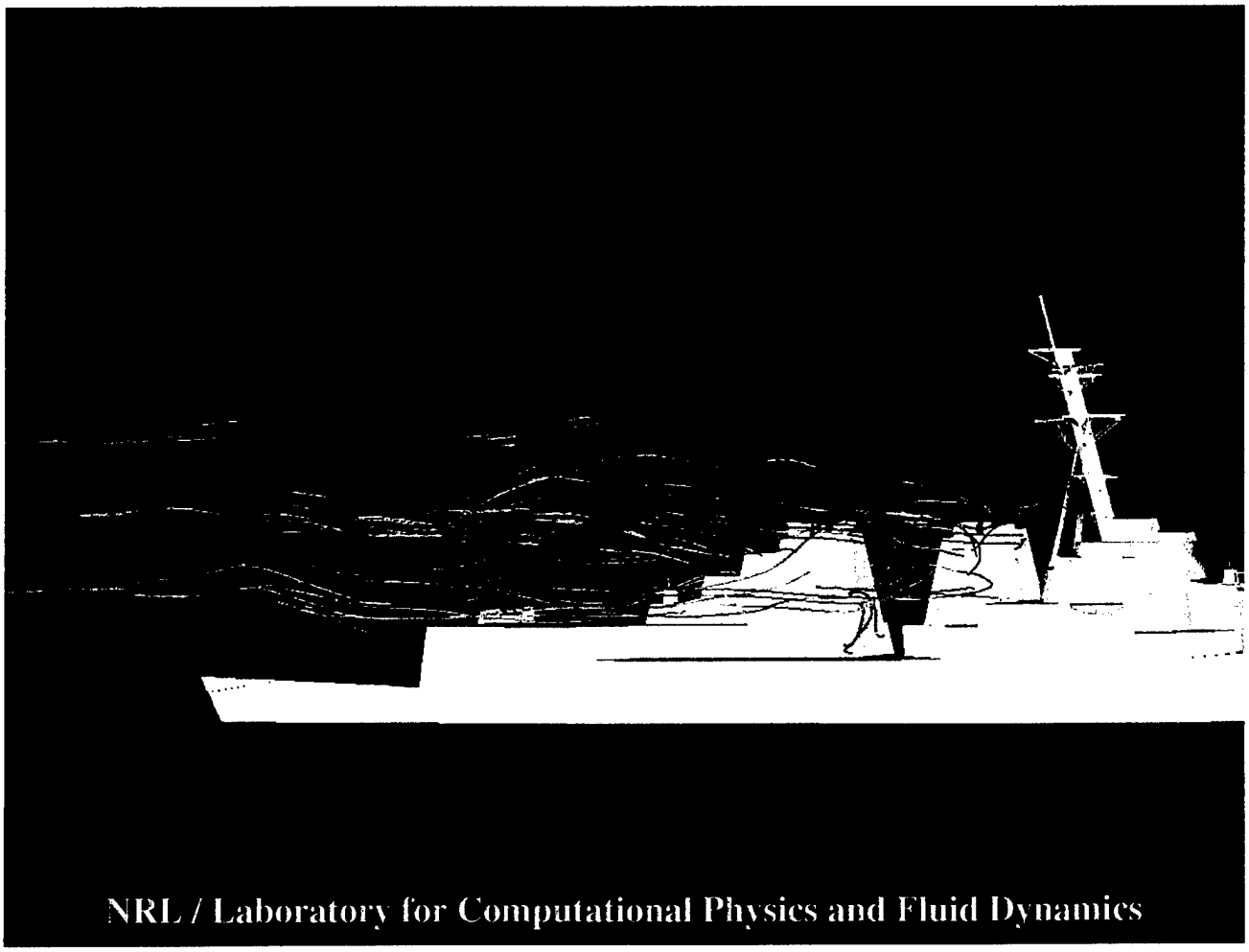
NRL / Laboratory for Computational Physics and Fluid Dynamics



Figure 6

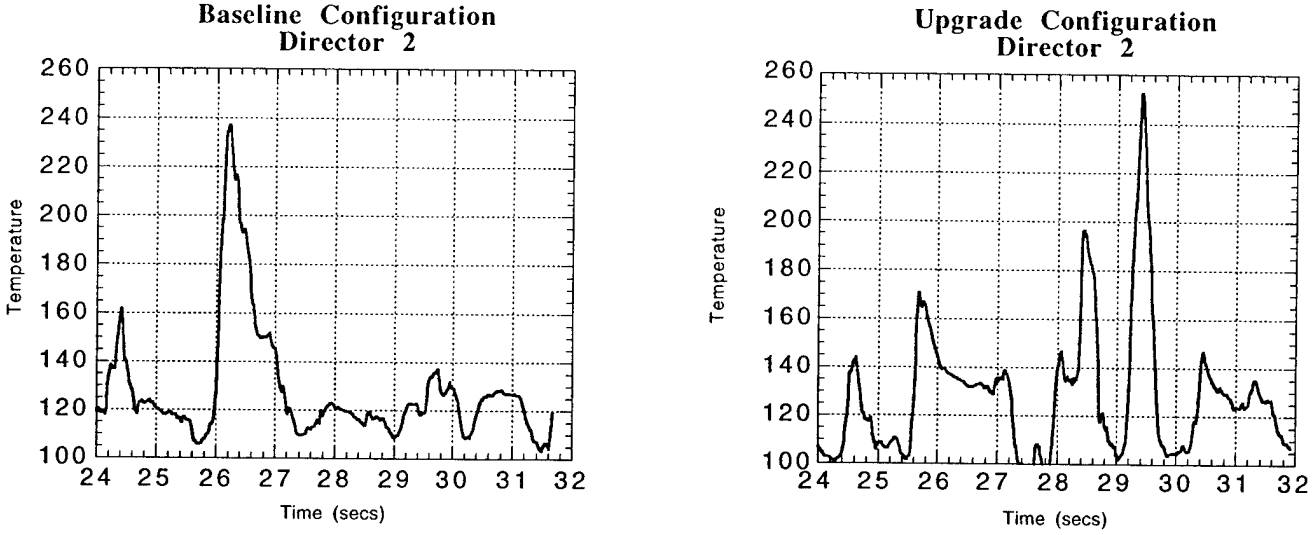


Figure 11. Temperature time history at Director 2 for (a) baseline configuration and (b) upgrade configuration for a 20 kt ship speed and 20 kt wind speed at 0° (headwind).

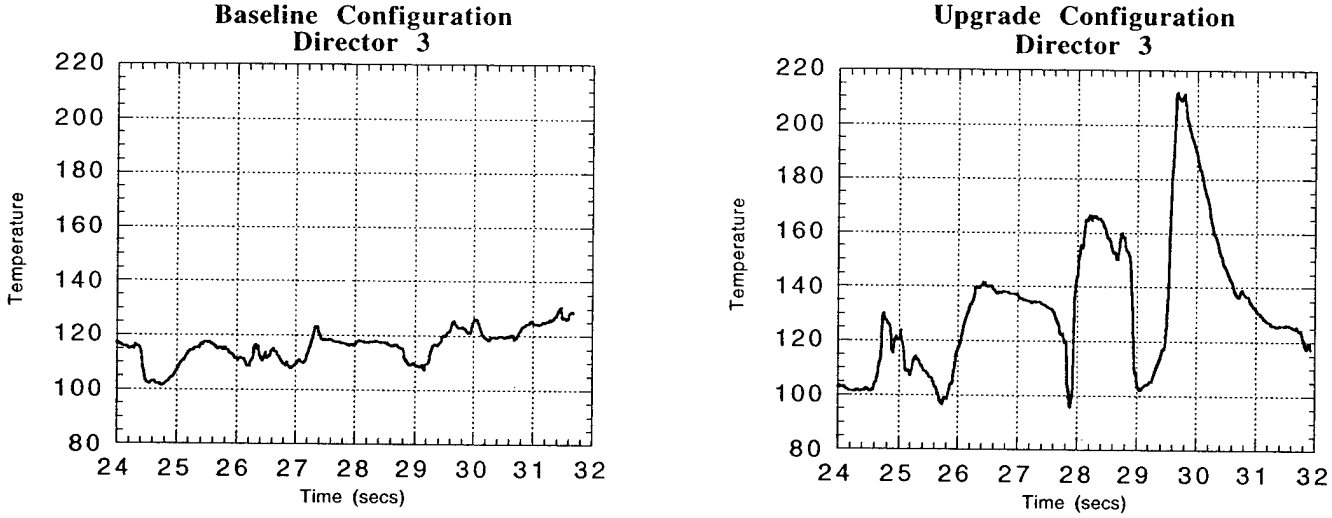


Figure 12. Temperature time history at Director 3 for (a) baseline configuration and (b) upgrade configuration for a 20 kt ship speed and 20 kt wind speed at 0° (headwind).

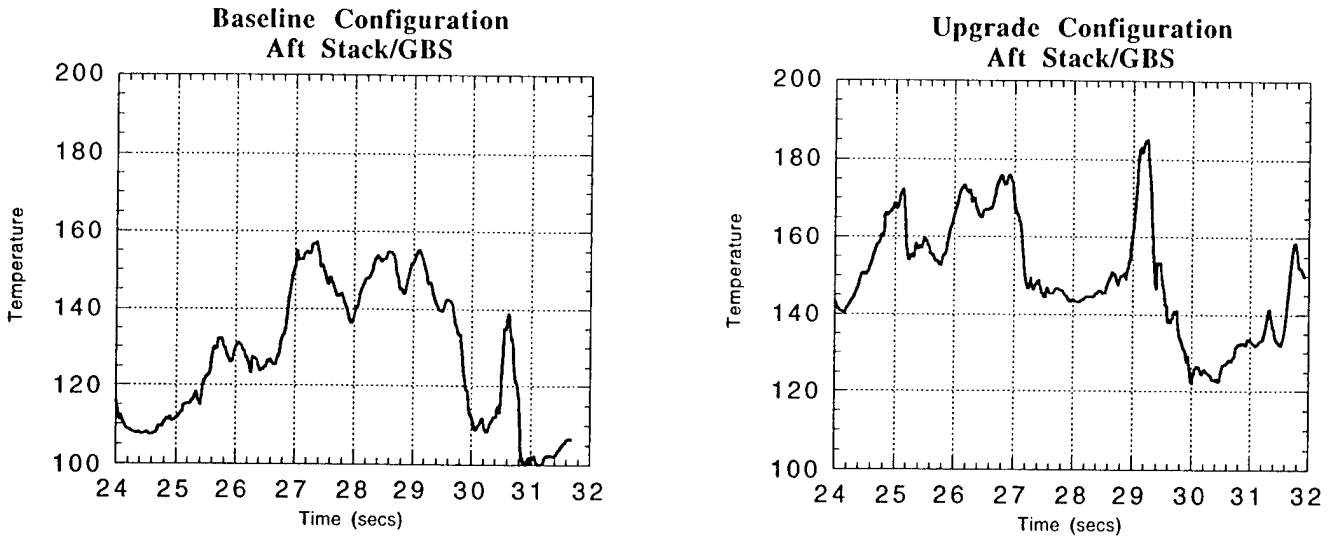


Figure 13. Temperature time history at Aft Stack/GBS for (a) baseline configuration and (b) upgrade configuration for a 20 kt ship speed and 20 kt wind speed at 0° (headwind).

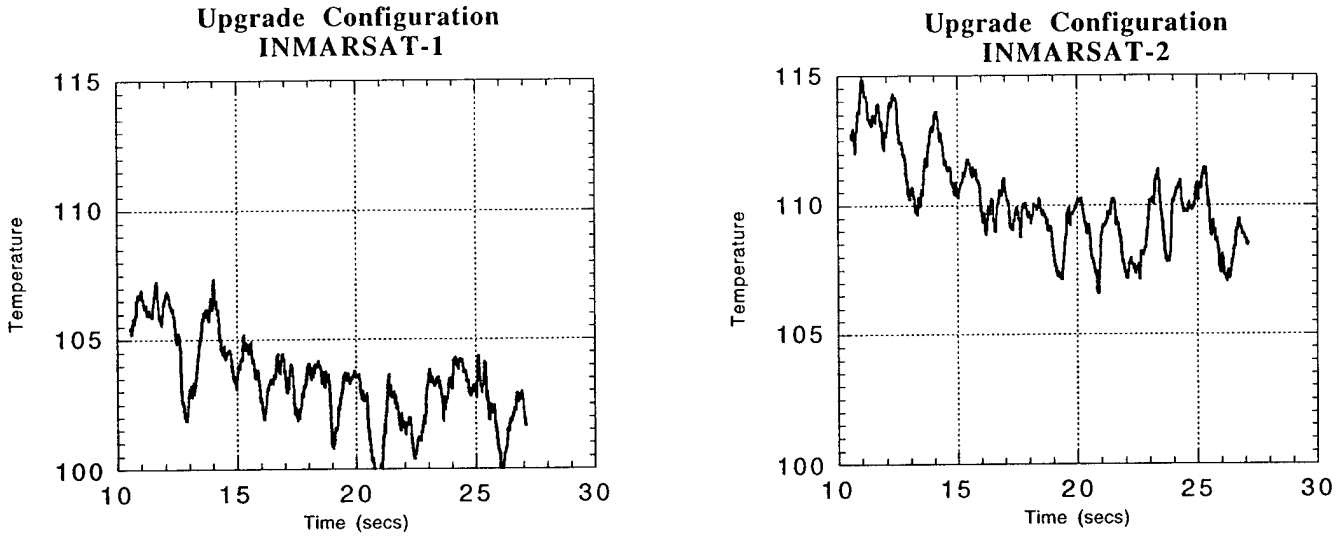


Figure 14. Temperature time history for baseline configuration at (a) INMARSAT-1 and (b) ) INMARSAT-2 for a 20 kt ship speed and 20 kt wind speed at 45°.

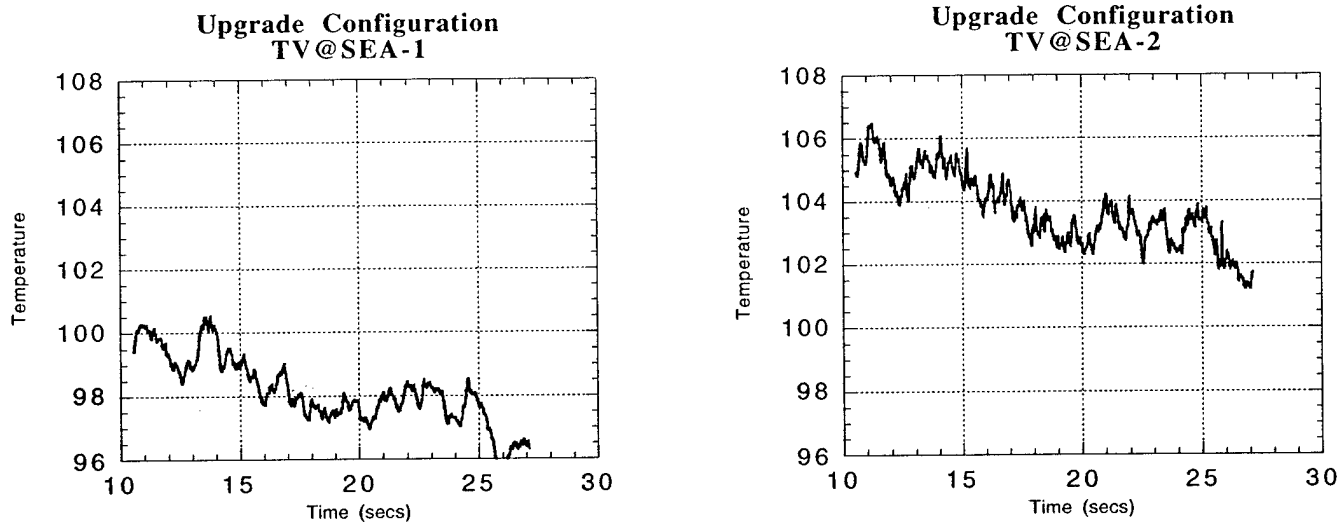


Figure 15. Temperature time history for baseline configuration at (a) TV@SEA-1 and (b) ) TV@SEA-2 for a 20 kt ship speed and 20 kt wind speed at 45°.

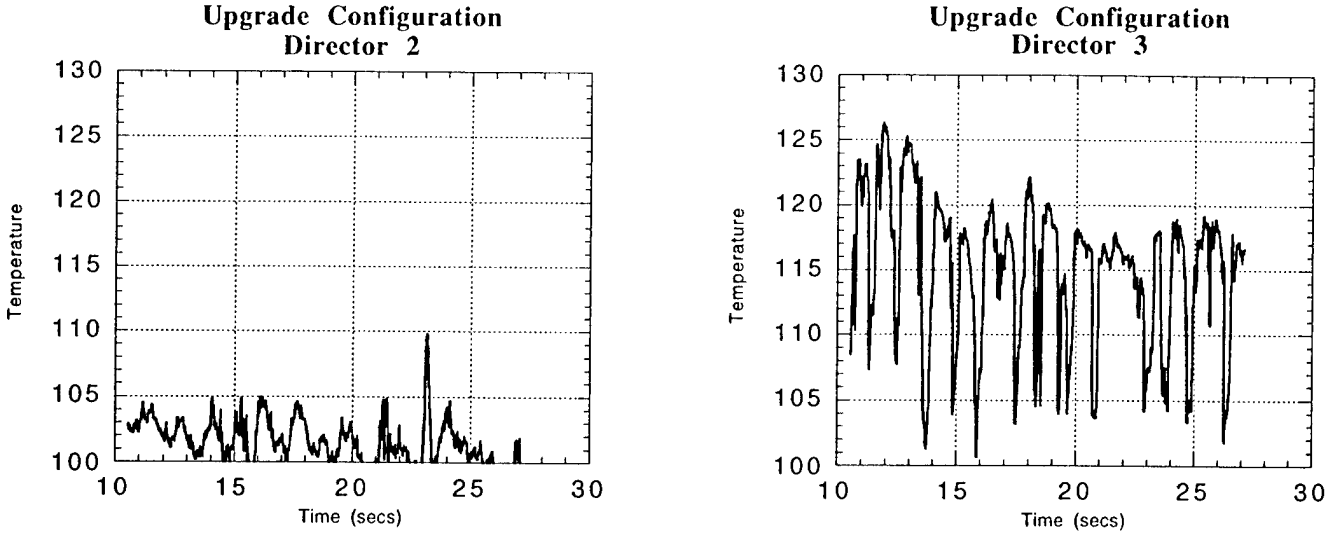


Figure 16. Temperature time history for baseline configuration at (a) Director 2 and (b) ) Director 3 for a 20 kt ship speed and 20 kt wind speed at 45°.

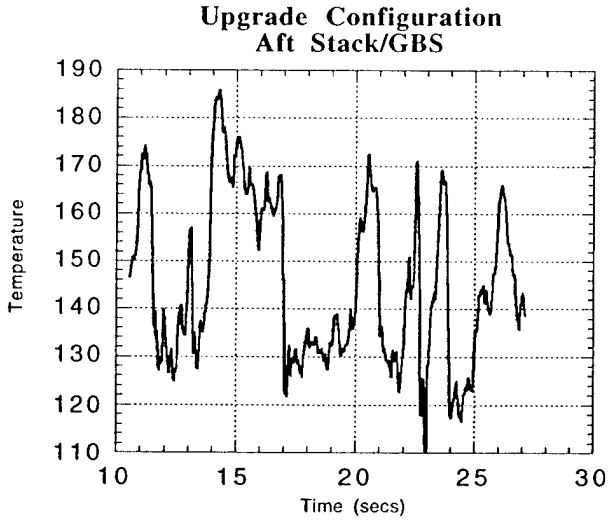


Figure 17. Temperature time history for baseline configuration at Aft Stack/GBS for a 20 kt ship speed and 20 kt wind speed at 45°.

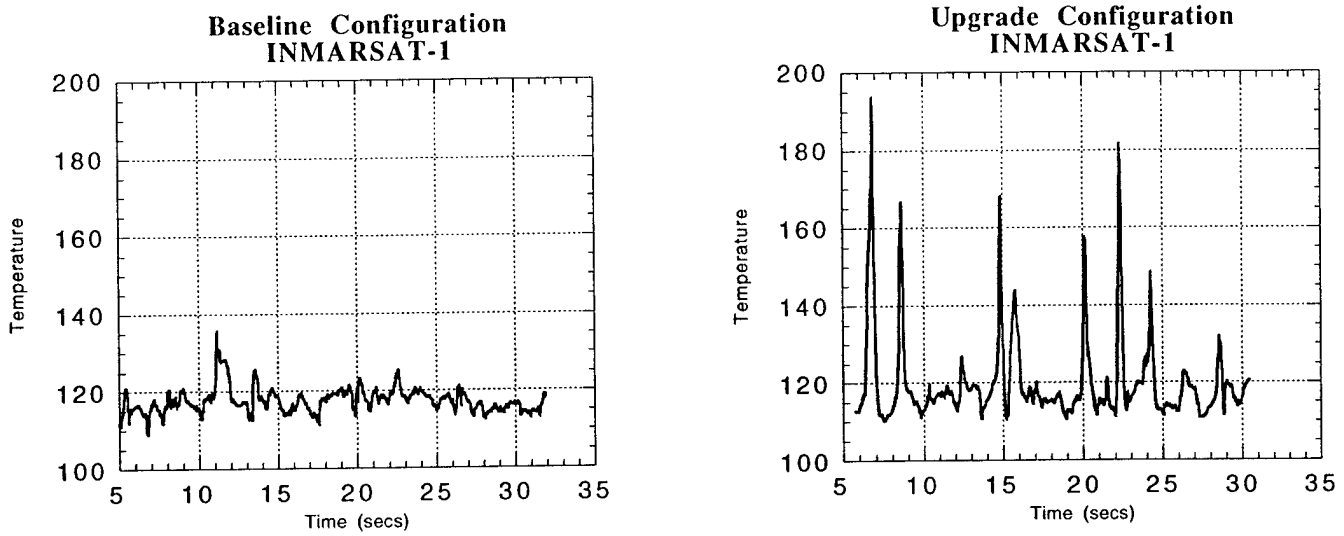


Figure 18. Temperature time history at INMARSAT-1 for (a) baseline configuration and (b) upgrade configuration for a 14 kt ship speed and 20 kt wind speed at 180° (tailwind).

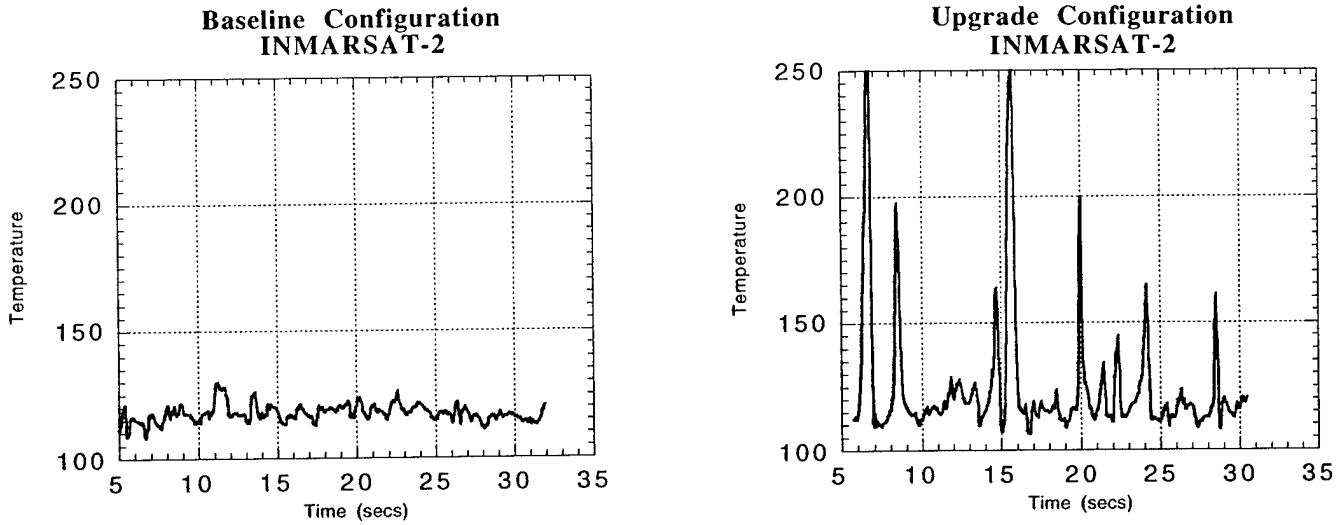


Figure 19. Temperature time history at INMARSAT-2 for (a) baseline configuration and (b) upgrade configuration for a 14 kt ship speed and 20 kt wind speed at 180° (tailwind).

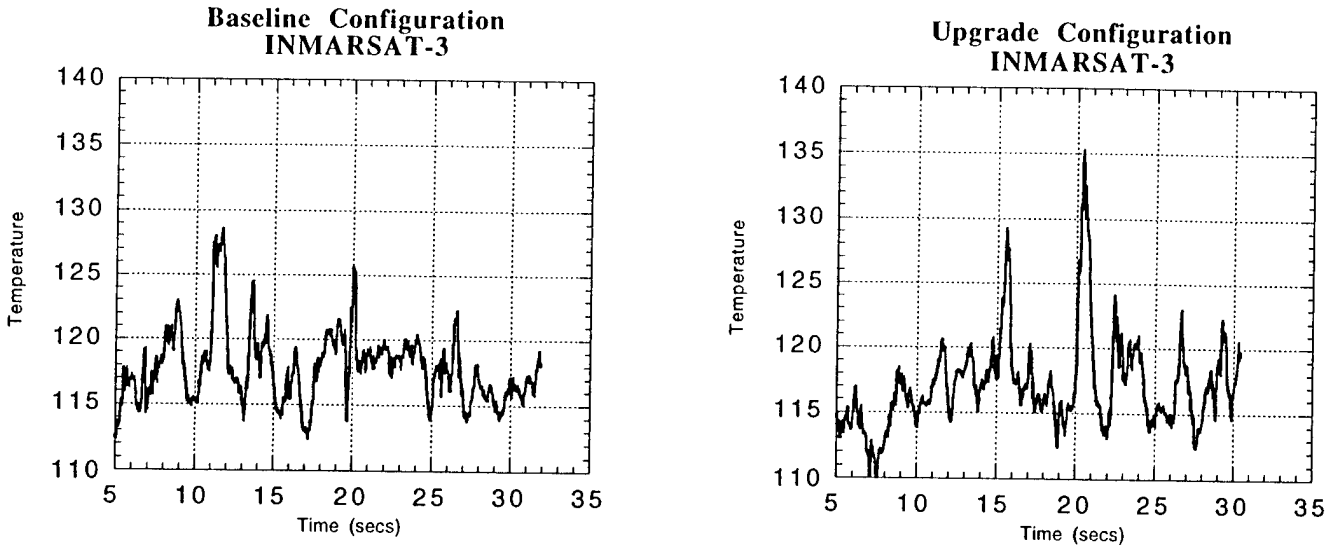


Figure 20. Temperature time history at INMARSAT-3 for (a) baseline configuration and (b) upgrade configuration for a 14 kt ship speed and 20 kt wind speed at 180° (tailwind).

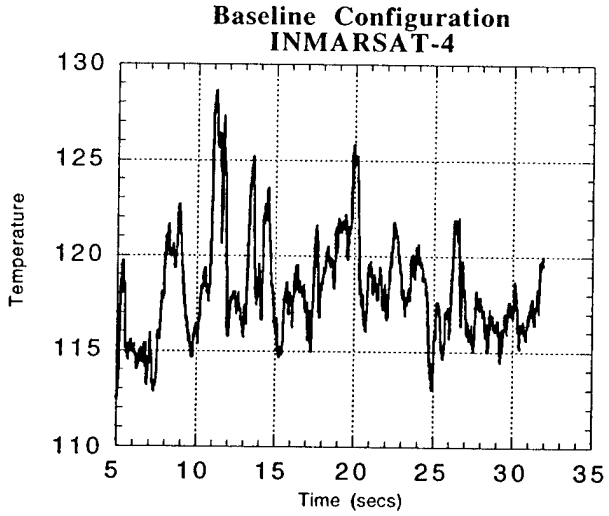


Figure 21. Temperature time history at INMARSAT-4 for (a) baseline configuration and (b) upgrade configuration (missing data) for a 14 kt ship speed and 20 kt wind speed at 180° (tailwind).

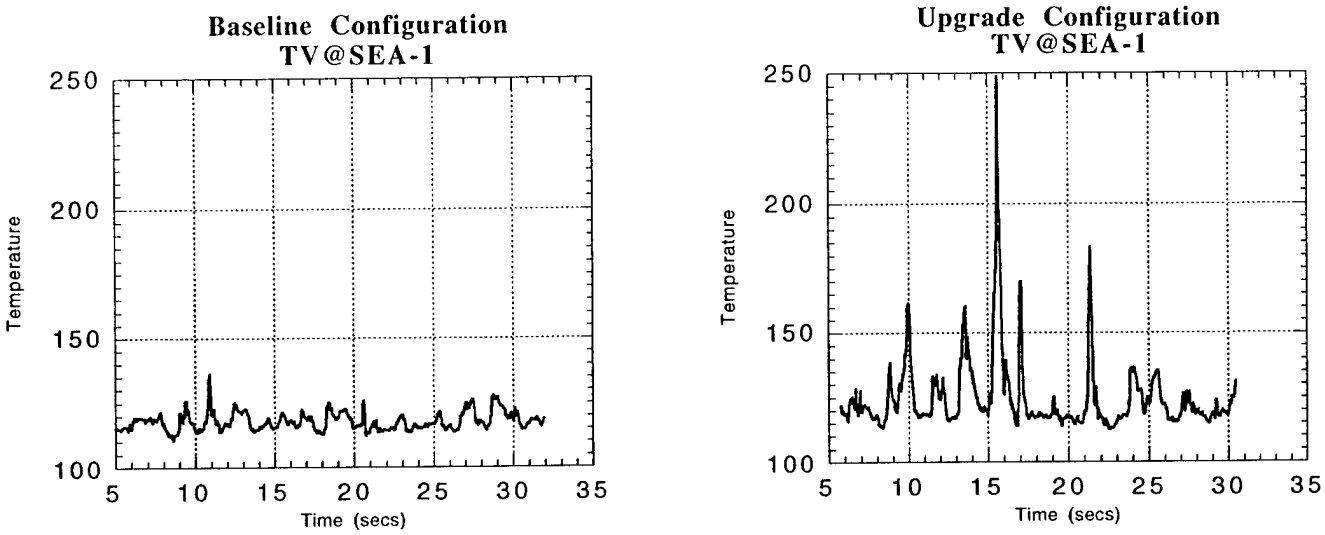


Figure 22. Temperature time history at TV@SEA-1 for (a) baseline configuration and (b) upgrade configuration for a 14 kt ship speed and 20 kt wind speed at 180° (tailwind).

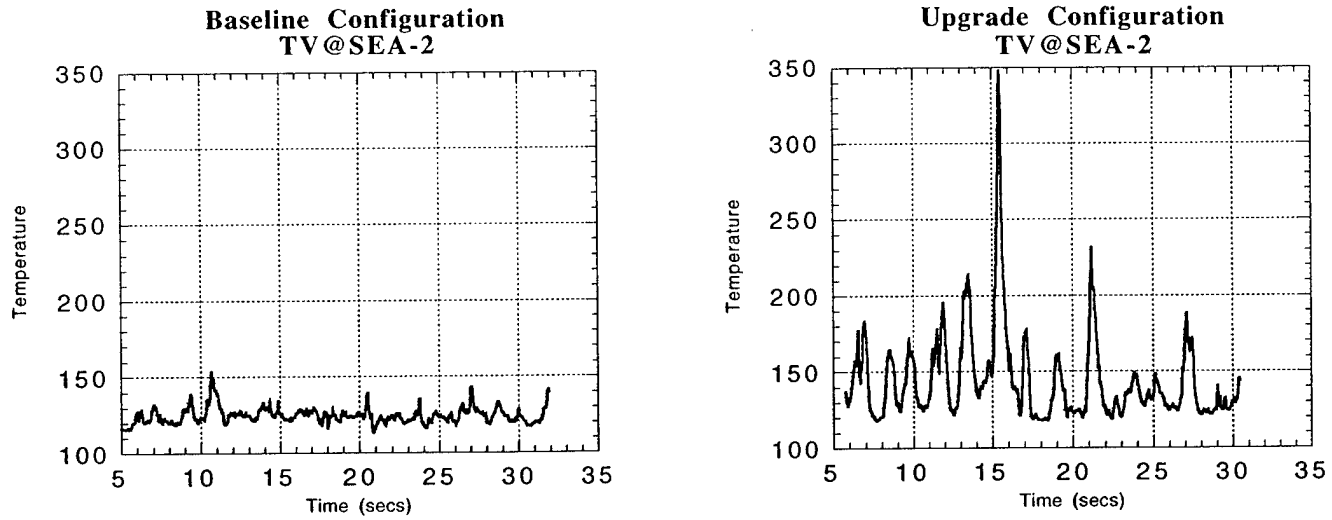


Figure 23. Temperature time history at TV@SEA-2 for (a) baseline configuration and (b) upgrade configuration for a 14 kt ship speed and 20 kt wind speed at 180° (tailwind).

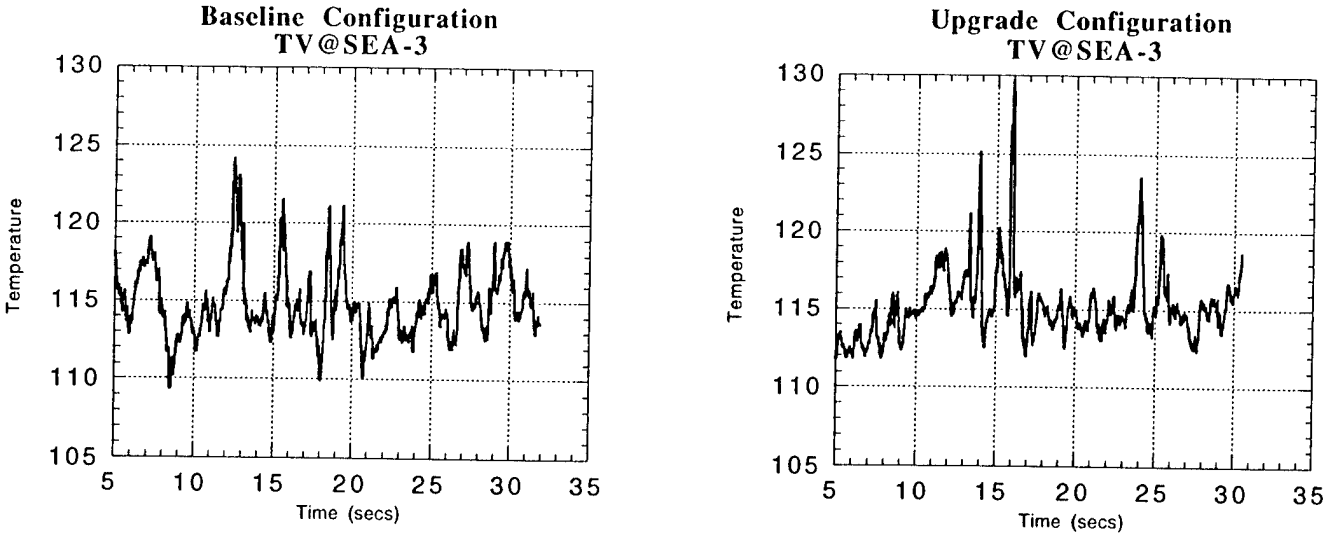


Figure 24. Temperature time history at TV@SEA-3 for (a) baseline configuration and (b) upgrade configuration for a 14 kt ship speed and 20 kt wind speed at 180° (tailwind).

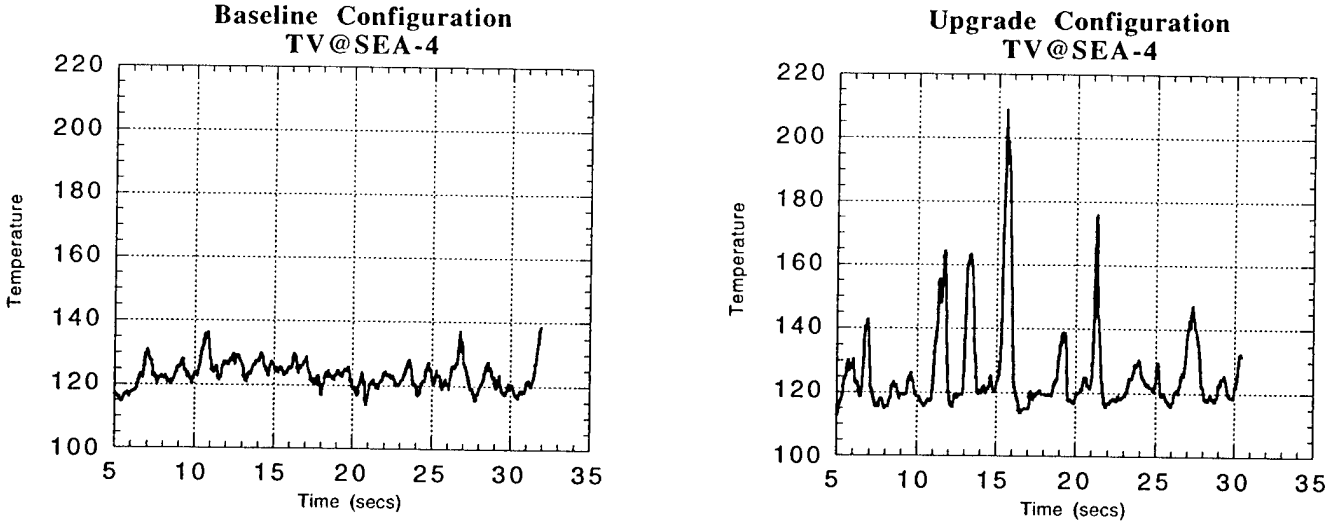


Figure 25. Temperature time history at TV@SEA-4 for (a) baseline configuration and (b) upgrade configuration for a 14 kt ship speed and 20 kt wind speed at 180° (tailwind).

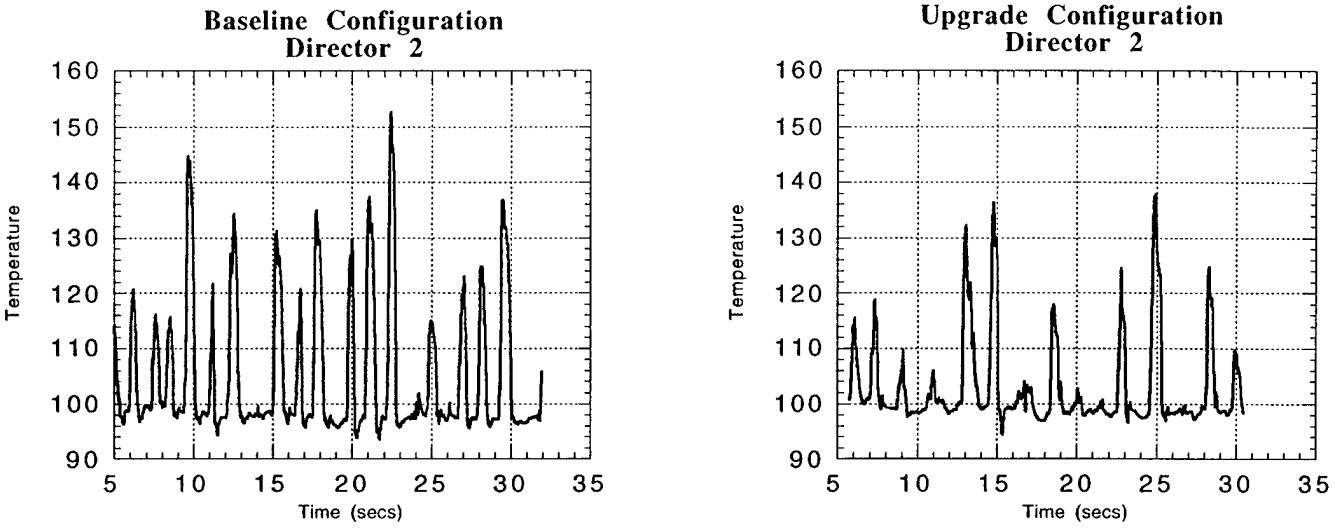


Figure 26. Temperature time history at Director 2 for (a) baseline configuration and (b) upgrade configuration for a 14 kt ship speed and 20 kt wind speed at 180° (tailwind).

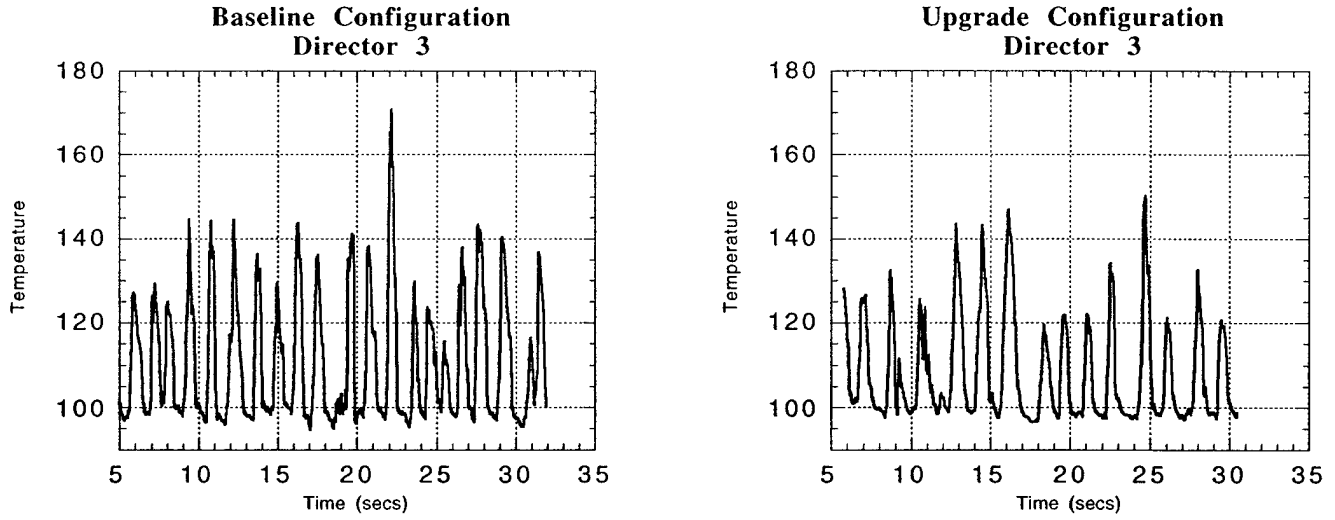


Figure 27. Temperature time history at Director 3 for (a) baseline configuration and (b) upgrade configuration for a 14 kt ship speed and 20 kt wind speed at 180° (tailwind).

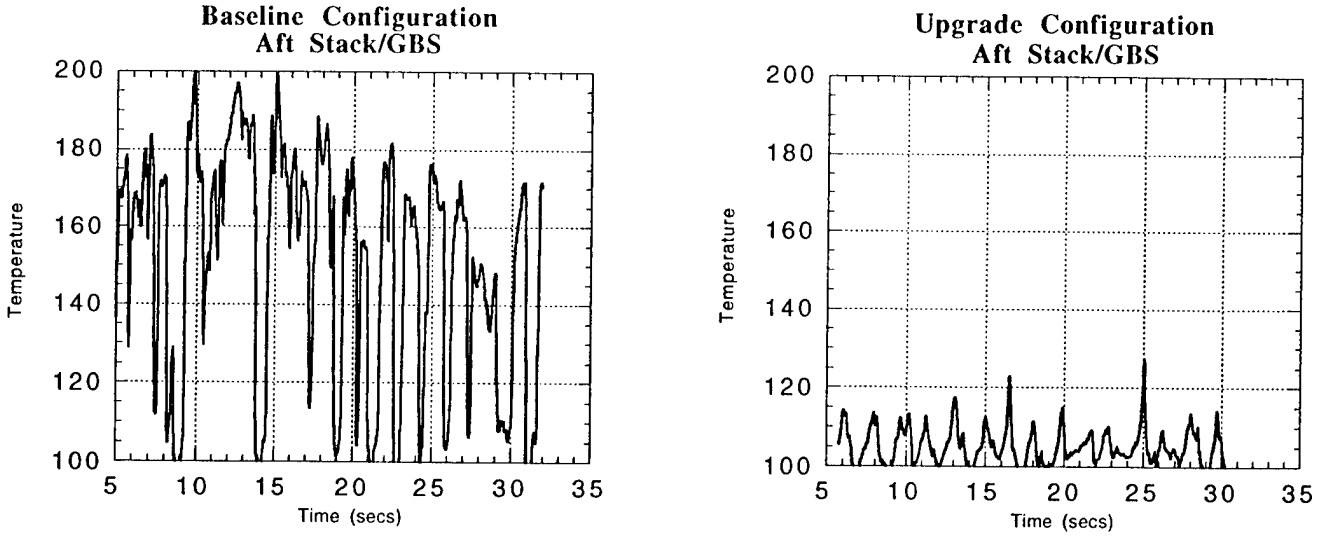


Figure 28. Temperature time history at Aft Stack/GBS for (a) baseline configuration and (b) upgrade configuration for a 14 kt ship speed and 20 kt wind speed at 180° (tailwind).

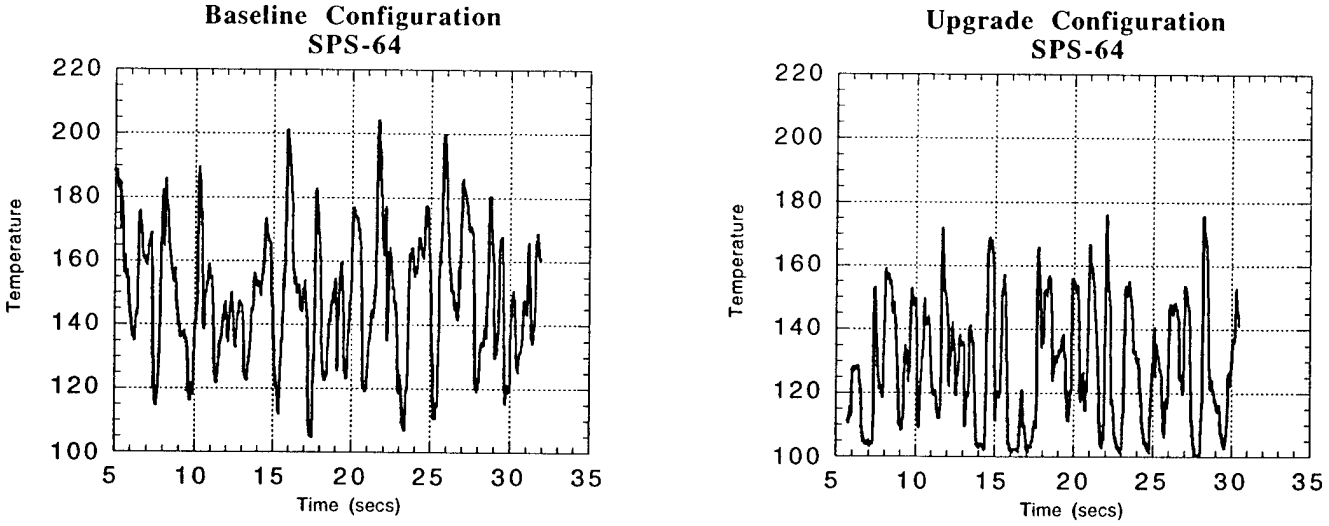


Figure 29. Temperature time history at SPS-64 for (a) baseline configuration and (b) upgrade configuration for a 14 kt ship speed and 20 kt wind speed at 180° (tailwind).

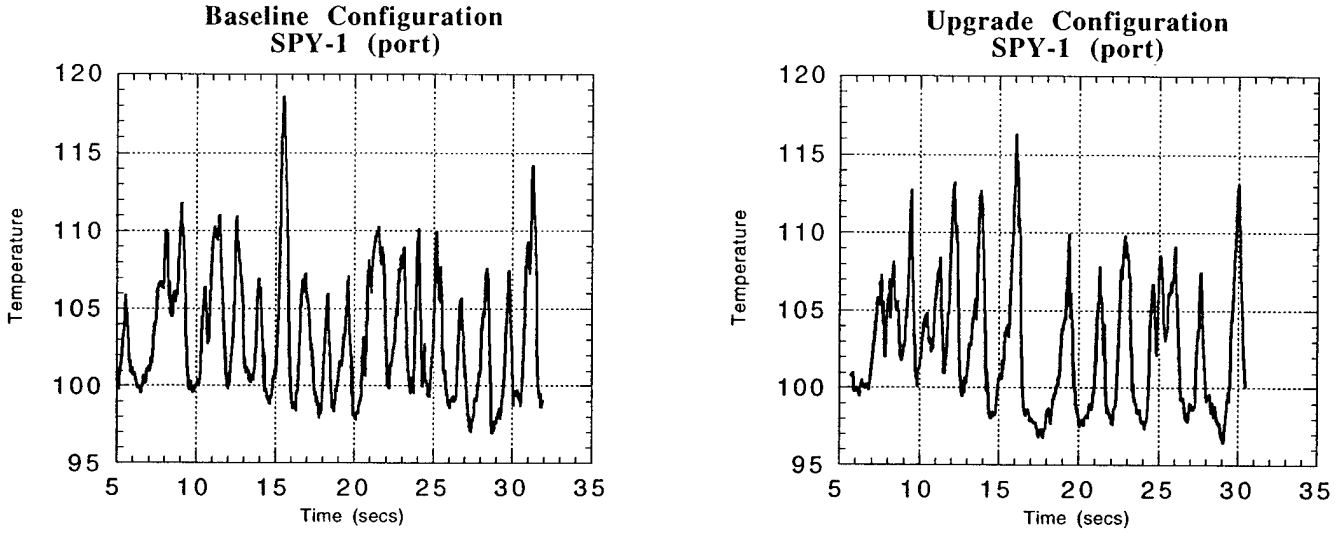


Figure 30. Temperature time history at SPY-1 (port) for (a) baseline configuration and (b) upgrade configuration for a 14 kt ship speed and 20 kt wind speed at 180° (tailwind).

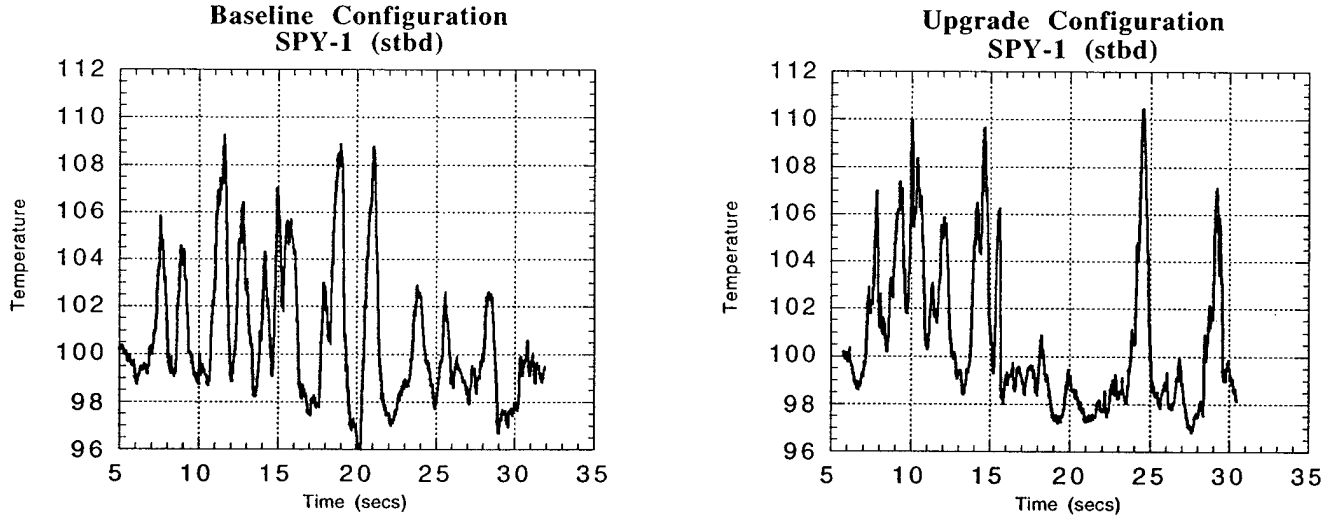


Figure 31. Temperature time history at SPY-1 (stbd) for (a) baseline configuration and (b) upgrade configuration for a 14 kt ship speed and 20 kt wind speed at 180° (tailwind).

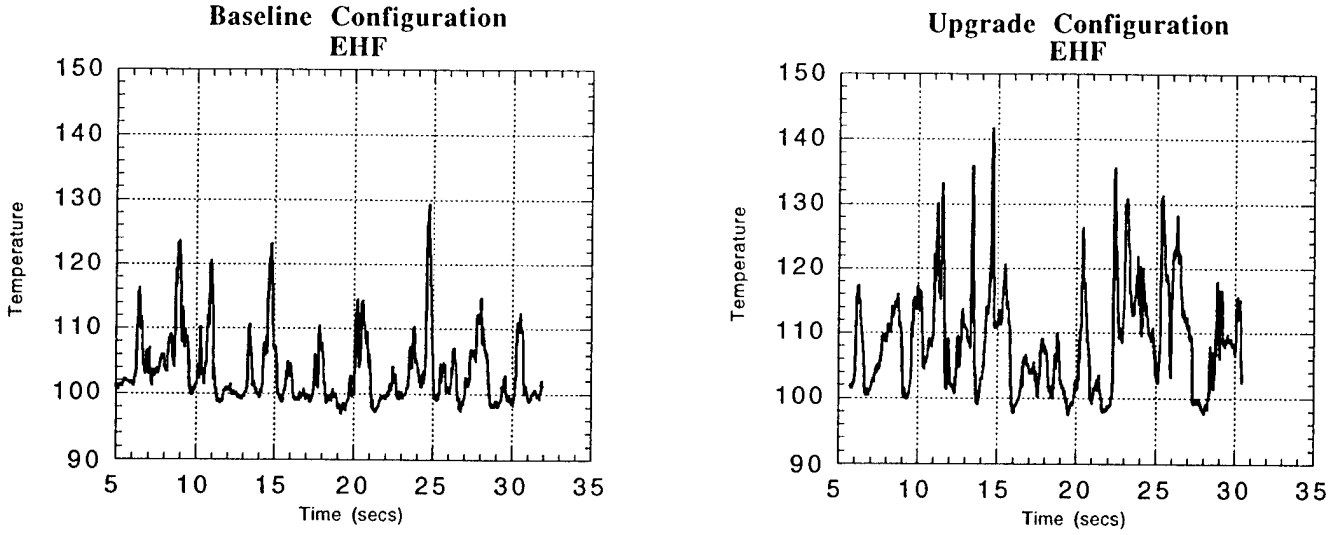


Figure 32. Temperature time history at EHF for (a) baseline configuration and (b) upgrade configuration for a 14 kt ship speed and 20 kt wind speed at 180° (tailwind).

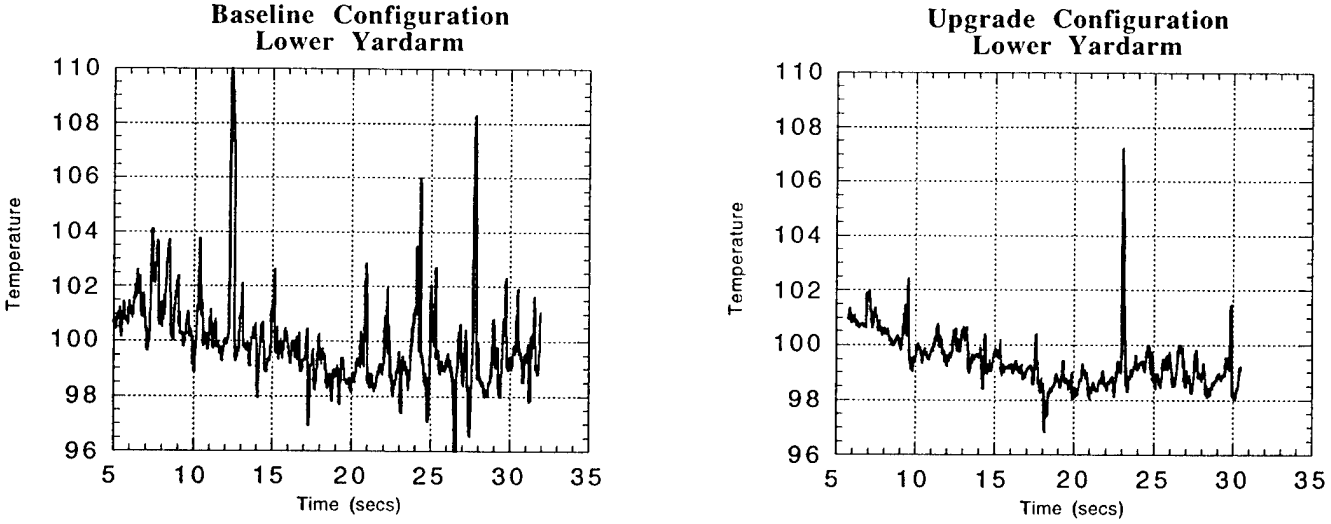


Figure 33. Temperature time history at Lower Yardarm for (a) baseline configuration and (b) upgrade configuration for a 14 kt ship speed and 20 kt wind speed at 180° (tailwind).

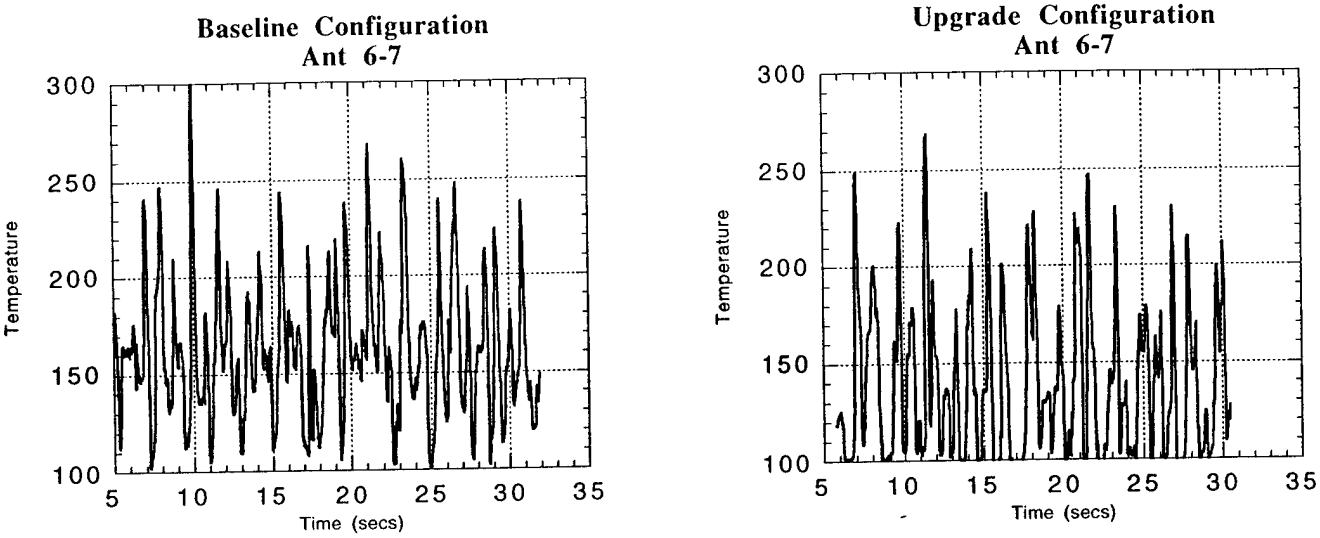


Figure 34. Temperature time history at Ant. 6-7 for (a) baseline configuration and (b) upgrade configuration for a 14 kt ship speed and 20 kt wind speed at 180° (tailwind).

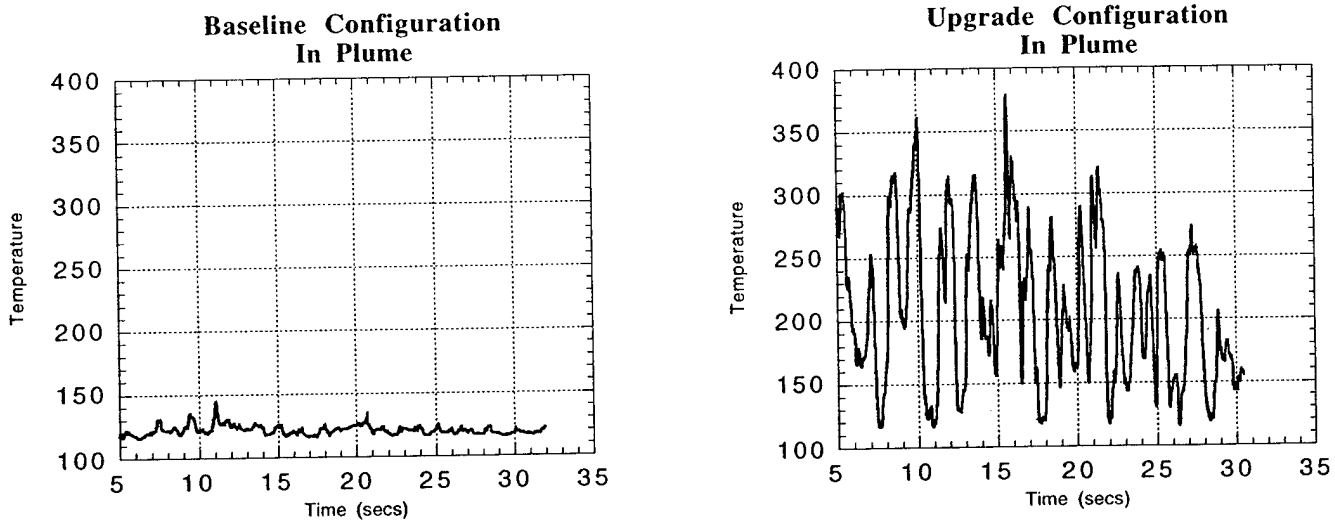


Figure 35. Temperature time history at location'In Plume'for (a) baseline configuration and (b) upgrade configuration for a 14 kt ship speed and 20 kt wind speed at 180° (tailwind).